DISSERTATION

LOCALIZATION OF PLASMA MEMBRANE PROTEINS IN LIPID RAFTS DURING SIGNALING

Submitted by

Steven M. L. Smith

Department of Biomedical Sciences

In partial fulfillment of the requirements

For the Degree of Doctor of Philosophy

Colorado State University

Fort Collins, Colorado

Summer 2006

COLORADO STATE UNIVERSITY

12 MAY, 2006

WE HEREBY RECOMMEND THAT THE DISSERTATION PREPARED UNDER OUR SUPERVISION BY STEVEN M. L. SMITH ENTITLED LOCALIZATION OF PLASMA MEMBRANE PROTEINS IN LIPID RAFTS DURING SIGNALING BE ACCEPTED AS FULFILLING IN PART REQUIREMENTS FOR THE DEGREE OF DOCTOR OF PHILOSOPHY.

Committee on Graduate Work

Advisor

Department Head

ABSTRACT OF DISSERTATION

LOCALIZATION OF PLASMA MEMBRANE PROTEINS IN LIPID RAFTS DURING SIGNALING

We have examined the preferential trafficking of membrane proteins to specialized, cholesterol-enriched microdomains within the plasma membrane termed lipid rafts. Isopycnic sucrose gradient ultracentrifugation was used to subfractionate membrane fragments. Membrane proteins of interest within low or high buoyant density membrane fractions were identified on Western blots prepared from sucrose fractions. To independently confirm these results, we used other methods including single-particle tracking to characterize the confinement of individual membrane proteins within small membrane compartments. In studies of the luteinizing hormone receptor (LHR), a receptor involved in male and female reproductive function, we demonstrated that the LHR moves into cholesterol-enriched lipid rafts upon binding of its physiological ligand, human chorionic gonadotropin (hCG). Only LHRs capable of receptor-receptor interactions translocate into these membrane structures. In studies of membrane proteins involved in allergen-mediated signaling in mast cells and basophils, we showed that the mast cell function-associated antigen (MAFA) is constitutively associated with the type I Fcε receptor (FcεRI) and that, upon crosslinking of either MAFA or FcεRI, these membrane proteins translocate together into rafts. Together these studies suggest that rafts may be physiologically-relevant membrane structures involved in cell signaling events mediated by these membrane proteins.

The role of protein aggregation within the plasma membrane in ligand-mediated signaling and tranlocation of membrane proteins into rafts is also discussed.

Steven M. L. Smith
Department of Biomedical Sciences
Colorado State University
Fort Collins, CO, 80523
Summer, 2006

TABLE OF CONTENTS

LIST OF FIGURES

LIST OF TABLES

CHAPTER 1

BACKGROUND

The plasma membrane is a dynamic structure that maintains cell integrity and regulates the internal environment of the cell. Many membrane functions are carried out by proteins that undergo movement and reorganization in the plane of the membrane. We are interested in the ability of membrane proteins to move between and within specialized compartments that exist in the plasma membrane. Simons and Ikonen coined the term, "lipid raft", to refer to a highly buoyant membrane fragment that "floats" in low density sucrose (1). Here we have characterized events leading to the retention of two membrane receptors, LHR and the high affinity FcεRI as well as a membrane glycoprotein, MAFA, which interacts with FcεRI and regulates its function in rafts.

Plasma membrane structure and organization

Singer and Nicholson proposed the fluid mosaic model of the cell membrane in the early 1970s. In their model (Figure 1), the two-dimensional phospholipid bilayer contains a mixture of proteins (2). Membrane lipids form amphipathic bilayers that surround cells to functionally block the leakage of hydrophilic compounds while also housing membrane proteins. There is diversity in the relative amounts of various membrane lipids and their structure, which typically consists of a polar head group and acyl chains. Eukaryotic cell

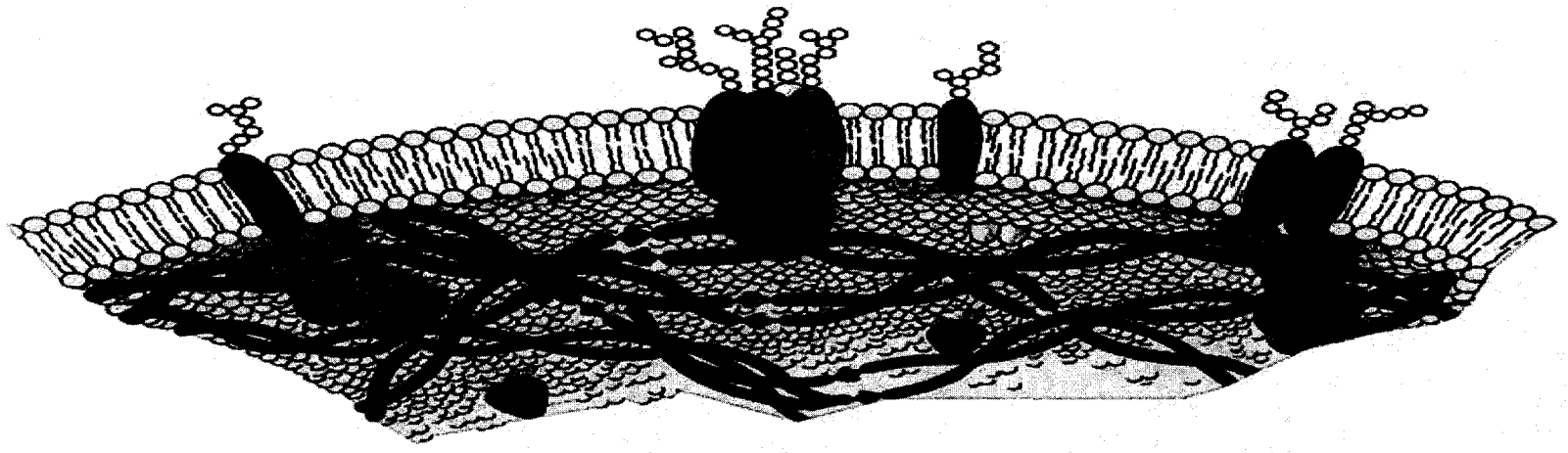

Figure 1: Membrane structure, modified from Stryer, Biochemistry, 4th edition (W. H. Freeman & Company, 1995).

membranes also contain spingolipids and sterols, such as cholesterol. One consequence of the lipid mixture is nonrandom segregation of lipids within the bilayer and the formation of lipid microdomains (3).

It was also generally appreciated from the Singer and Nicolson model that membrane proteins, which can be either integral membrane proteins embedded in the lipid bilayer or peripheral membrane proteins, can move within the plane of the membrane. In 1974, the lateral diffusion of a protein, rhodopsin within the frog visual membranes, was measured by Poo and Cone (4). Since then, the movement, distribution and localization of proteins within the membrane has been actively studied. In 1976, Axelrod and coworkers(5) developed an optical approach to measure the lateral diffusion coefficient of membrane proteins which they called fluorescence photobleaching recovery (FPR). This provided the groundwork for analysis of the recovery of fluorescence after photobleaching of a fluorescent probe. In a typical FPR experiment, an attenuated laser beam was focused onto a fluorochrome-labeled cell membrane as observed in a fluorescence microscope. After recording of initial fluorescence intensity for several seconds using an attenuated laser beam, a few millisecond pulse of laser light intense enough to cause significant photobleaching was applied. The attenuated beam was then used to monitor the diffusion of unbleached fluorophores into the interrogated spot. Analysis of fluorescence recovery after photobleaching using non-linear curve fitting techniques revealed the diffusion coefficient and fractional mobility of the cell surface protein being observed.

Working independently, Jacobson and coworkers (6) developed a similar method, giving it the name most commonly used today, fluorescence recovery after photobleaching

(FRAP). Examples of early work using FPR or FRAP include contributions from the Barisas group (7) who introduced photobleaching measurements on lymphocytes and by Ware's group (8) who examined oligomerization of actin filaments. The development of intrinsically fluorescent receptors using visible fluorescent proteins (VFP) has greatly facilitated the use of microscope-based methods for characterizing lateral movement of proteins and protein-protein interactions. Many researchers now use GFP to study the localization of fusion proteins in living cells and also, with FRAP methods to study protein dynamics and activity within a single living cell (9).

There is increasing evidence that membrane proteins may move within and between membrane compartments and that the trafficking of proteins involved in, for example, signal transduction, may be important to protein function (10, 11). Baird and coworkers (12) have demonstrated that native, monomeric FcεRI receptors occupied by IgE are localized mainly within the "bulk" plasma membrane regions. Upon binding of antigen by IgE, upwards of 50% of the total receptor population is found in membrane fragments called "rafts" that float into lower density sucrose within sucrose concentration gradients. Oh and co-workers (13) have shown that certain members of the heterotrimeric G protein family, namely G_s and G_i, are preferentially trafficked to lipid rafts by default(13). Glycosylphosphotidylinisitol (GPI)-anchored membrane proteins are markers for raft domains (14). They are concentrated at the apical surfaces of polarized epithelial cells both *in vitro* and *in vivo* (15). Horejsi and coworkers have isolated GPI-anchored proteins from human lymphocytes using cold Triton X-100 (16). These proteins were part of detergent-insoluble complexes that included src family tyrosine family kinases. The referenced studies are the basis for a large body of

literature that generally shows association of ligated receptors, signaling kinases and phosphatases, and G proteins that form signaling complexes within raft fractions (17).

Based on these and other observations, there has been increased interest in membrane heterogeneity and, in particular, in rafts. Lipid rafts is a descriptive term describes the detergent-resistant membrane fractions that partition in sucrose density gradients within fractions that were different from those containing the bulk of membrane proteins. Most evidence supporting rafts comes from studies of membrane fragments that are insoluble in cold, non-ionic detergents such as Triton X-100. Arguments have been made that the raft association of proteins is driven by, or an artifact of, detergent-based homogenization of the cell membrane constituents. There has been as much discussion about whether rafts truly exist or are experimental artifacts as there has been about their functions (18).

Nonetheless, Simons and Ikonen (1) suggest that there are complex interactions between cholesterol, sphingolipids and other molecules including phosphatidyl choline and that these interactions may be responsible for lipid raft structure. The sphingolipids and cholesterol may pack very tightly together between regions that are usually occupied by unsaturated phosphatidylcholine molecules to produce the large, cholesterol-enriched, cluster. Further evidence for rafts comes from chemically sequestering cholesterol using methyl-β-cyclodextrin (MβCD). MβCD depletes cholesterol from the plasma membrane without disrupting the membrane or causing cell death. This treatment disrupts rafts and can decrease receptor-mediated signaling in raft structures containing necessary intermediaries in signaling pathways. Moreover, careful MβCD treatment, while rapidly and efficiently depleting the cholesterol from living cells, does not compromise cell viability (19).

(20). Members of this receptor superfamily regulate cell homeostasis, growth and reproductive functioning among other biological signaling pathways. Family members have seven membrane-spanning domains and the ability to dock with the heterotrimeric G proteins in the plasma membrane. Hydropathy analysis of the primary sequence of all GPCRs predicts seven membrane-spanning α helices connected by three intracellular loops and three extracellular loops with an extracellular amino terminus and an intracellular carboxy terminus. This basic structure has now been verified by x-ray crystallography for rhodopsin (21). Although there was already evidence that visual transduction in the retina and hormone activation of adenylyl cyclase shared common features, the discovery that the β-adrenergic receptor has the same topographic structure as rhodopsin came as a surprise (22). Cloning of the complimentary deoxyribonucleic acids (cDNAs) for a vast number of GPCRs followed elucidation of the primary sequence of the β-adrenergic receptor and, in every case, the same core structure was predicted by hydropathy analysis. The rhodopsin crystal structure identifies the residues in the transmembrane helices that interact with retinal and suggests a mechanism for movement of the helices upon photoactivation of retinal (21) which in turn lead to changes in the conformation of cytoplasmic loops and G protein activation.

One member of this receptor superfamily is the LHR, a seven transmembrane domain-containing membrane receptor involved primarily in reproduction. LHR has a single polypeptide chain containing 674 amino acid residues, 340 of which make up the large, N-terminal extracellular domain which is extensively glycosylated. The seven transmembrane

domains consist of 24 amino acids each and the intracellular C-terminal tail is 70 amino acids long (23, 24). Because it is a single peptide chain, there are three extracellular and intracellular loops connecting the seven transmembrane domains, as shown in Figure 2. Rat LHRs have extensive glycosylation and, as a result, the cell surface receptor demonstrates a native molecular weight of approximately 85-95 kDa (23).

Two hormones are able to bind to the luteinizing hormone receptor, luteinizing hormone (LH) and human chorionic gonadotropin (hCG). These hormones are members of the glycoprotein hormone family that includes LH and hCG as well as follicle stimulating hormone (FSH) and thyroid stimulating hormone (TSH). Both LH and hCG exist as heterodimers consisting of one α and one β subunit and are assembled by non-covalent interactions (25). Both subunits are required for high affinity binding to LHR. The α subunit, a 92-96 amino acid peptide, is highly conserved for LH and hCG as well as the other glycoprotein hormones. Specific to each hormone, and demonstrating more variability, is the β subunit which confers receptor specificity. The β subunit of LH contains 117 amino acids while the β subunit for hCG has 142 amino acids (26).

LHRs participate in both male and female reproductive functions. The reproductive system requires hormone-mediated communication between the hypothalamus and the anterior pituitary which results in release of hormones from the anterior pituitary, including LH, that produce desired effects on cells within the gonads, which is illustrated in Figure 3. Each part of the system has a well-defined role, starting with the release of the 10 amino acid peptide hormone gonadotropin releasing hormone (GnRH) by secretory neurons in the hypothalamus into the hypophyseal circulation. In the anterior pituitary, the GnRH binds to

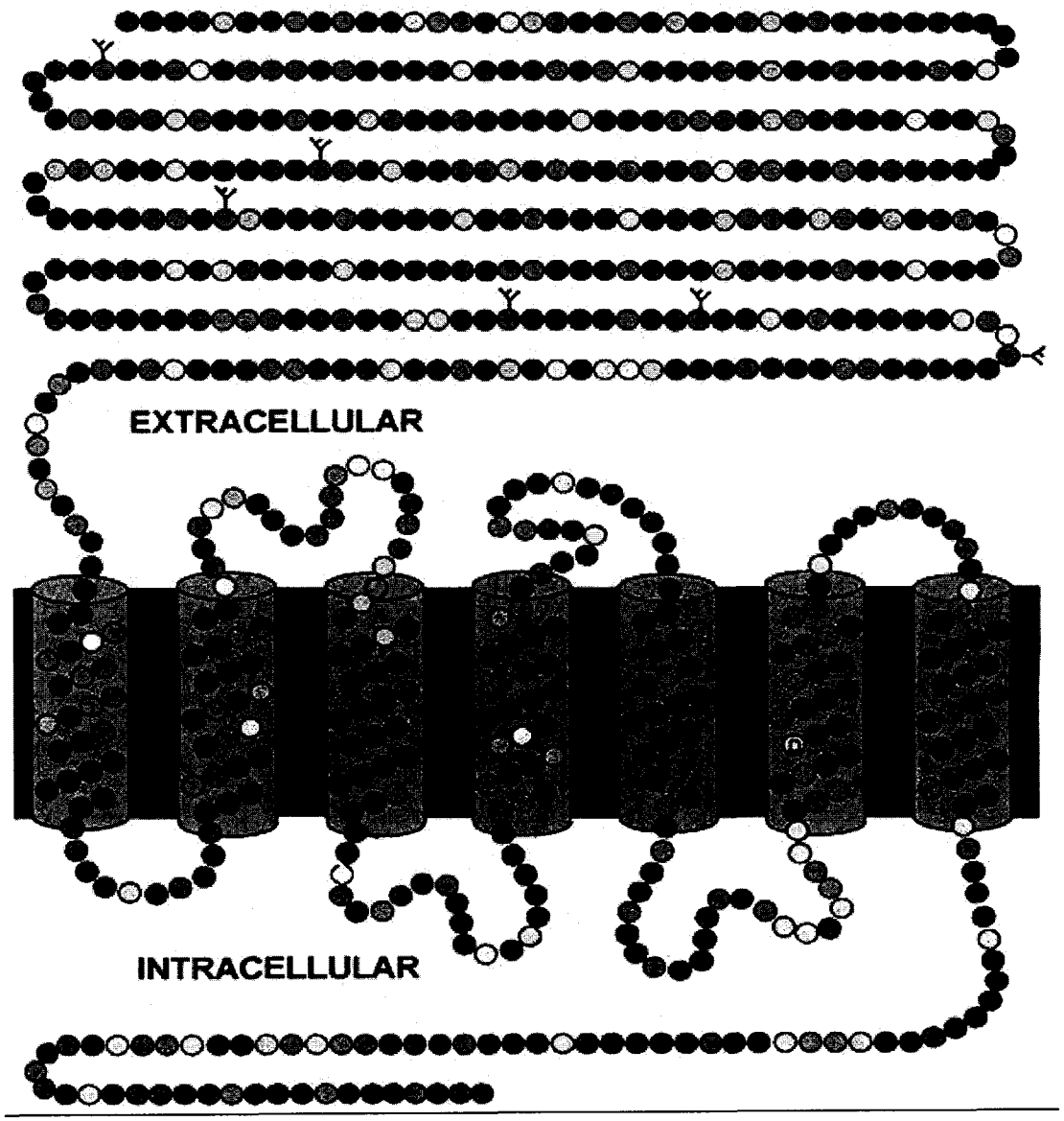

Figure 2: LH receptor organization from McFarland et al (22).

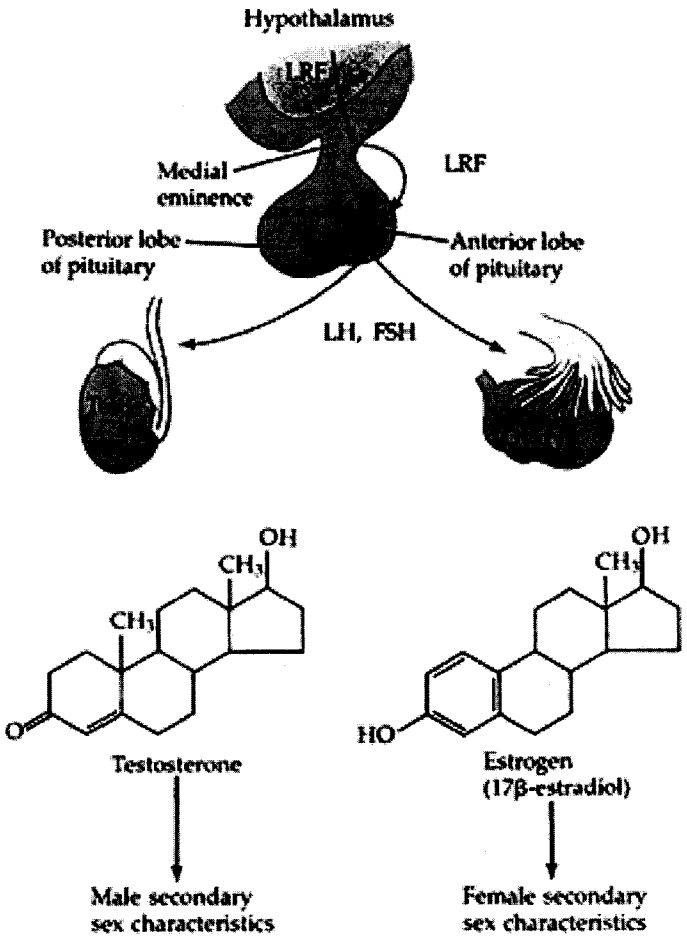

Figure 3: Hypothalamic-pituitary-gonadal axis in mammalian reproductive physiology. Adapted from Gilbert, Developmental Biology, 7th edition (2003, Sinauer Associates, Inc.).

the GnRH receptor which, like LHR, is a G protein-coupled receptor. GnRH binding to its receptor on gonadotrophs located in the anterior pituitary drives these cells to synthesize and secrete LH into the systemic circulation. LH then binds to its receptor in the testes or ovaries where it will lead to tissue-specific sex steroid hormone synthesis and release (27). Synthesis and secretion of LH is, like many signaling systems in the body, tightly controlled. In the nonpregnant female, LH released from the anterior pituitary drives production of estradiol by ovarian follicular cells. Estradiol, provides feedback signals at both the central and pituitary levels. The system is further modulated by three additional peptide hormones, inhibin, activin and follistatin (28).

LHRs play an important role in this system and must function properly in both males and females for normal reproduction. In females, LHR serves two functions, both essential for successful reproduction. At approximately day 14 in the menstrual cycle, LH spikes, binding to LHRs on theca interna and follicular cells, initiating events leading, within approximately thirty-six hours, to ovulation. The second LHR function in humans occurs early in pregnancy. Following fertilization, a placentally-derived structure, the chorion begins to synthesize and secrete hCG in increasingly large quantities. hCG binds to LHRs on the corpus luteum which leads to the continued production of progesterone, the hormone responsible for maintenance of the uterine lining, particularly in early pregnancy. As such, hCG signaling is essential for retention of the pregnancy. Production of hCG by the syncytiotrophoblast reaches its maximum by the tenth week of pregnancy, but is maintained at a low but readily measurable level for the duration of the pregnancy.

In males, LH is responsible for many important functions, including embryonic

sexual differentiation, development of the testes and normal functioning of the Leydig cells, including testosterone production. During fetal development, LHR on Leydig cells bind LH. These cells then secrete testosterone which drives growth and development of the male reproductive tract structures, including penis, prostate, and epididymis. After puberty, Leydig cells will begin to produce more testosterone in response to LH and that will lead to the development of the secondary sex characteristics such as increased muscle mass, pubic and facial hair, voice deepening and sperm production by the testes.

Signal transduction by LHR

LHR-mediated responses occur as a result of signal transduction following binding of either LH or hCG to the receptor. The LHR is a G protein-coupled receptor, with a relatively high affinity for its ligand. Despite the tremendous diversity in G protein-coupled receptors, only about twenty G proteins act as intermediaries between receptors and the intracellular signal transduction machinery (29). There are three subunits that make up the G proteins, coded for by three distinct genes. The α-subunit binds guanine nucleotides with high affinity and specificity and has intrinsic GTPase activity. The β and γ polypeptides are tightly, but not covalently, associated in a functional dimer subunit. There is some diversity in G protein subunits, with no fewer than 16 distinct α-subunit genes in mammals. One ubiquitous variant is Gs-α, which couples many GPCRs to stimulation of adenylyl cyclase. This conservation of G proteins means that there is "lock and key" specificity between ligands and receptors but promiscuous binding between activated receptors and available G

proteins. Activation of the LHR causes the heterotrimeric Gs to dissociate into α, β and γ subunits, with the α subunit acting on adenylyl cyclase. Adenylyl cyclase, a membrane protein and identified G protein-regulated effector, enzymatically converts adenosine monophosphate into cyclic AMP. Mediators of second messenger metabolism such as adenylyl cyclase, as well as phospholipase C and a variety of ion channels thus alter intracellular concentrations of important second messengers and ions. The results can be rapid effects on hormone secretion, muscle contraction and a variety of other physiologic functions. This process is summarized in Figure 4.

Additionally, a protein, arrestin, has been implicated in the attenuation of signaling, as initially described for the retinal photoreceptor, rhodopsin (30). Just as parallels were discovered between rhodopsin and GPCR structure, so were parallels identified in this desensitization mechanism (31). Arrestin is one member of a family of related proteins that function in desensitization of many members of the GPCR superfamily. There is evidence that arrestins and other proteins function not only in receptor desensitization but also to mediate other functions including receptor internalization (32).

Signaling by the LHR is, as discussed earlier, carefully regulated. However, in Familial Male-limited Precocious Puberty (FMPP), a dominant mutation results in constitutive activation of the LHR (33) and therefore overproduction of the second messenger cyclic adenosine monophosphate (cAMP). Unoccupied, mutant receptors drive cAMP accumulation, causing Leydig cell hyperfunction and, in some cases, tumor formation (34). The naturally-occurring mutations affect thirteen different residues in LHR, with the majority clustered in the cytoplasmic half of transmembrane helix six. Again, similar to

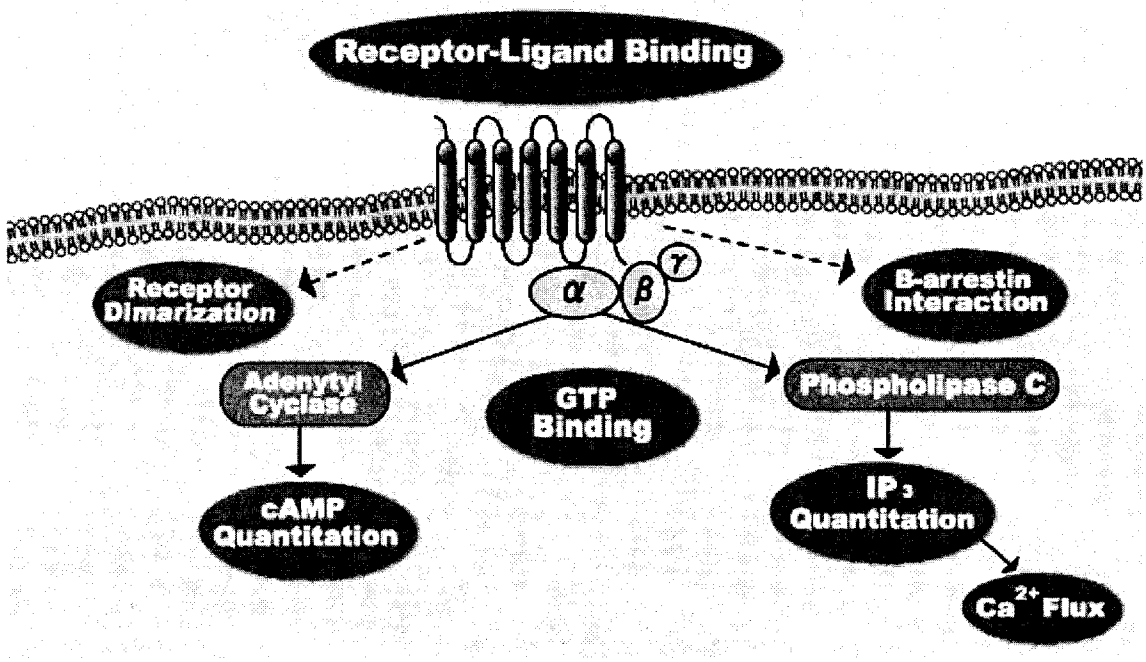

Figure 4: G protein-coupled receptor signaling pathways. Modified from Perkin-Elmer product literature, 2006.

rhodopsin, conformational signaling appears to depend on the rearrangement of key electrostatic, hydrogen-bond, and hydrophobic interactions that normally serve to stabilize the inactive LHR conformation (33).

One event that is important in signal transduction is self-association between functional receptors and even large scale clustering within the plasma membrane following hormone binding (35). Signal transduction by LHRs requires a change in receptor organization from an isolated, monomeric state to an aggregated, associated state (36). This can be demonstrated in viable cells using fluorescence resonance energy transfer (FRET) methods. LHRs were coupled to either green fluorescent protein (GFP) or yellow fluorescent protein (YFP) and these receptors were co-expressed in Chinese hamster ovary (CHO) cells. Activation of the receptors by hCG led to a measurable increase in intracellular cAMP and also FRET between receptors (37). These FRET results indicated that receptors were in fact within 100Å of each other after being activated by a hormone (38). Using human LHR constructs in which CFP and YFP molecules were coupled to the receptor C-terminus, fluorescence dequenching FRET was evaluated between two receptors. Exciting one molecule with a laser led to characteristic emission of light by the other molecule in the pair only when hormone was also present, again suggesting that the two receptors are within 100Å (37) during the signaling process (39). Interestingly, constitutively active receptors were also constitutively associated with one another in the absence of hormone (38).

Interactions between FcεRI and MAFA

Plasma membrane receptors are also involved in immune system functions. One group of immunoreceptors, the Fc receptors, bind the Fc domains of immunoglobulin IgE isotype with a stoichiometry of 1:1. Binding by itself does not initiate degranulation of mast cells or basophils; rather clustering of Fc receptors via the bound IgEs which serve as antigen-specific, divalent adapters, provides the signal leading to the above cellular response (40). Basophils are an important experimental system for studying the events coupling Fc receptors to cellular responses. These cells respond instantly to clustering of FcεRIs by secreting their granules' contents, a process which can be quantitatively monitored (41, 42). The commonly-employed and stable rat mucosal-type RBL-2H3 basophilic leukemia-derived cell line has $3\text{-}6x10^5$ FcεRI per cell and these bind IgE with nanomolar affinity (43). Clustering the FcεRI initiates a cascade of biochemical processes leading to secretion of granule-stored mediators such as histamine (44) and the *de novo* synthesis and secretion of arachidonic acid metabolites (45) and of several cytokines (46, 47). The coupling cascade includes recruitment and activation of specific protein tyrosine kinases (48). This in turn causes a transient increase in tyrosine phosphorylation of several cellular proteins (49, 50).

The structure of the high affinity IgE receptor, the FcεRI is well characterized. One alpha (α) chain, one beta (β) chain and two identical disulfide-linked gamma (γ) chains make up the functional receptor which is a tetrameric protein. The receptors are monovalent and bind monomeric IgE molecules with a Ka of about 10^{10}M (51). Aggregation of the FcεRI is essential for its function, and to demonstrate this, intact antibolies to the α subunit are able

to trigger the degranulation response in mast cells, but their Fab fragments are not. In addition, the FcεRI was one of the first membrane receptors to be studied in relation to its localization within the plasma membrane when signaling, and more specifically, whether it was actively signaling in lipid raft domains. Dr. Barbara Baird and her colleagues have shown that significant fractions of the total number of aggregated receptors co-purify with rafts following sucrose gradient ultracentrifugation (12). Additionally, the Baird lab has demonstrated that the cholesterol sequestering agent methyl-β-cyclodextrin (MβCD) can disrupt the structure of lipid rafts, tyrosine phosphorylation of the FcεRI and also disrupt its association with Lyn, a signaling intermediary (52).

Another membrane component that is an active participant in the allergen-mediated degranulation response by mast cells was originally identified by Dr. Israel Pecht. His lab identified and characterized a glycoprotein on the surface of rat basophilic leukemia cells (RBL-2H3 cells) and named it the MAst-cell-Function-associated Antigen, or MAFA (53). This type II transmembrane glycoprotein was shown to have significant sequence homology with several members of the C-type (calcium-dependent) animal lectin family. Their lab has produced a monoclonal antibody designated G63 to the MAFA protein, that, when bound to MAFA on RBL-2H3 cells, significantly attenuated the classic allergen-mediated degranulation by the FcεRI. Interestingly, the MAFA protein is expressed at considerably lower levels that is the FcεRI, 10-20 fold fewer copies of MAFA per cell. Even so, the binding of G63 to MAFA leads to approximately a 50% decrease in histamine released in response to an allergen. Structural diagrams of the FcεRI and MAFA appear in Figure 5.

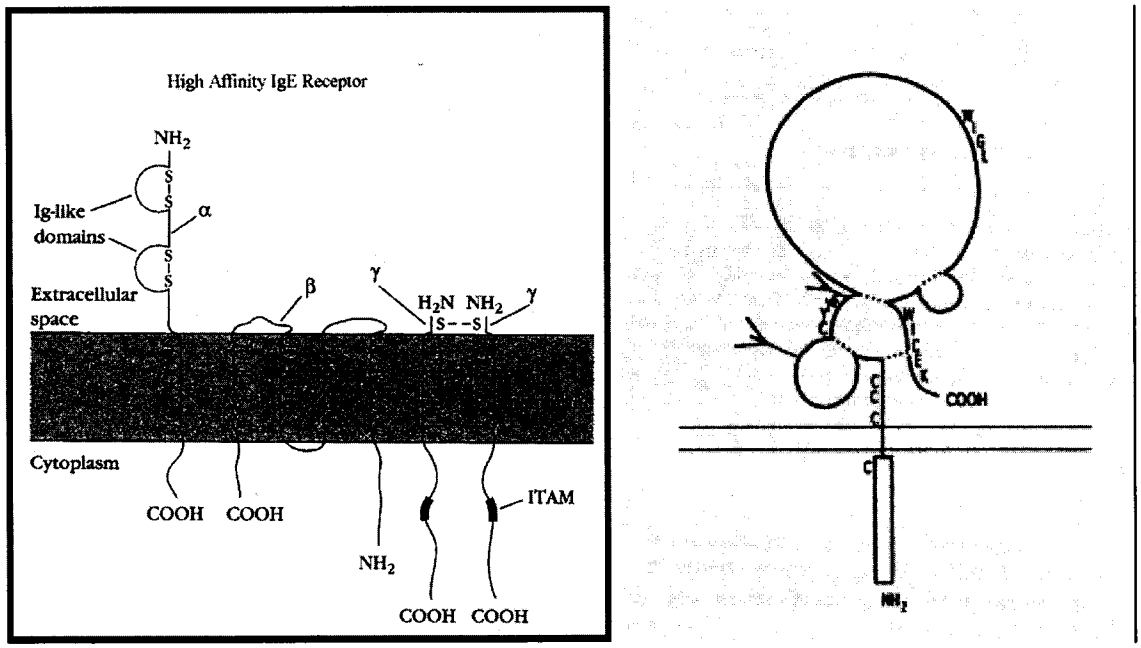

FcεRI MAFA

Figure 5: Structure of FcεRI and MAFA. The FcεRI contains seven transmembrane domains, composed of four subunits. Immunoreceptor tyrosine activation motifs (ITAMs), phosphorylation targets of Lyn, are found on the receptor γ chains. MAFA is a single membrane-spanning protein (134) with immunoreceptor tyrosine inhibitory motif (ITIM) on N-terminus (not indicated on diagram).

Compartmentalization of membrane proteins

There are a number of different experimental strategies that can be used to demonstrate localization of membrane proteins in small membrane compartments. Plasma membrane rafts are identified biochemically using an established method to isolate cholesterol-rich membrane fragments from the rest of the bulk plasma membrane. Following TX-100 lysis and sucrose gradient ultracentrifugation, proteins of interest such as LHR, FcεRI and MAFA are tracked through the gradients by Western blotting of carefully collected fractions following isopycnic ultracentrifugation. Typically, a 40% sucrose cut-off is used to separate raft fractions from bulk plasma membrane fractions which segregate to sucrose concentrations containing ≥ 40% sucrose. Because the raft microdomains are enriched with cholesterol, depletion of cholesterol using MβCD disrupts these structures and produces a redistribution of raft components to membrane fragments with low buoyancy.

A microscope-based strategy for examining compartmentalization of individual proteins involves tracking of these proteins on viable cells. In single-particle tracking experiments, a 40 nm colloidal gold molecule is attached to an antibody or other lipid- or protein-specific probe. The motions of individual proteins or lipids can be monitored over time and analyzed for particle lateral diffusion and the size of compartments accessed by the membrane molecule can be determined (54). This technique has shown that proteins can exhibit various types of motion including random Brownian diffusion, directed motion due to active transport, constrained random motion and immobilization (55). A single protein molecule can change its behavior in response to, for example, hormone-binding to its

membrane receptor while lipids continue to diffuse freely in the plasma membrane of spreading and locomoting cells.

Small compartments are often required for sustained interactions between membrane proteins and disruption of the compartment leads quickly to disaggregation of interacting proteins. Examining interactions between proteins in small compartments can be accomplished through a laser-optical method, time-resolved phosphorescence anisotropy (TPA), which evaluates the rotational correlation times of membrane proteins (56). These measurements have the advantage of being performed on intact cells under nearly physiological conditions. Rotational behavior of membrane proteins is a sensitive reflection of molecular size since the rotational correlation time (RCT) of anisotropy decay is linearly proportional to the molecule's in-membrane volume (57). If, for example, MAFA is constitutively associated with the FcεRI, then TPA measurements on the MAFA-FcεRI system should demonstrate that MAFA has the same apparent rotational correlation time as the FcεRI and this value should be larger than expected for an isolated molecule of MAFA's size (58). Furthermore, aggregating either FcεRI or MAFA into large clusters should rotationally immobilize both MAFA and the receptor, thus increasing the limiting anisotropies of both species. Lastly, crosslinking of a known raft component, membrane ganglioside GM1 (59), with cholera toxin should trap these proteins within rafts.

We will use various experimental strategies to determine whether aggregation of LHR accompanying ligand-mediated signaling is also associated with changes in compartmentalization of the receptor. Chapter 2 focuses on early studies describing the translocation of LHR into membrane rafts and the development of our working model for

LH-mediated signaling by this receptor. In Chapter 3, raft localization of LHR is explored in more detail with additional characterization of LHR retention in small membrane compartments using single-particle tracking methods. In Chapter 4, we take several approaches to examining interactions between FcεRI and MAFA which, from previous studies of protein rotational diffusion (60), appear to be constitutively associated with one another and characterize the translocation of these molecules into membrane microdomains. The co-localization of these molecules in small compartments suggests a possible mechanism by which MAFA, upon activation with G63 antibody, is able to effectively inhibit FcεRI-induced degranulation of cells in response to antigen crosslinking.

CHAPTER 2[1]

Self-Association and Raft Localization of Functional Luteinizing Hormone Receptors

Membrane motions of LH receptors following binding of hormone agonists are consistent with hormone-driven aggregation

It is increasingly apparent that G protein-coupled receptors, including the luteinizing hormone receptor, are engaged in dynamic interactions with one another and with other membrane components. These interactions are governed, in part, by a number of factors, including whether the receptor is bound to a ligand, whether the receptor is capable of transducing a hormone-mediated signal and the nature of the membrane environment within which the receptor is found. Microscopic methods, including laser-optical techniques, are ideally suited to probe dynamic events on cell membranes and provide an opportunity to examine interactions between receptors and other membrane components on viable cells. We and others have used a variety of techniques, some of which are summarized below, to examine functional and non-functional LH receptors on viable cells and the membrane environment of these receptors during cell signaling events.

The ability of an LH receptor to bind ligand and transduce signal directly affects the

---

1

This chapter has been adapted from Deborah A. Roess and Steven M.L. Smith (2003) Self-association and raft localization of functional luteinizing hormone receptors, *Biology of Reproduction* **69**:1765-1770.

types of interactions evoked by the receptor. LH receptor function can be substantively altered by several strategies including deleting portions of the receptor, substituting amino acids within the receptor, or binding a non-functional ligand such as deglycosylated hCG to the receptor. Functional LH receptors bind hormone agonists and produce measurable increases in levels of downstream signaling molecules such as cyclic AMP. Non-functional hormone-receptor complexes include receptors that have bound hormone antagonists or receptors that remain uncoupled from signal transduction machinery despite binding of hormone agonists. To determine whether the membrane environment of non-functional hormone-receptor complexes differed qualitatively from that of functional hormone-receptor complexes, we compared the rotational dynamics of various complexes on 293 cells using time-resolved phosphorescence anisotropy methods.

Because the rotational diffusion of membrane proteins is linearly related to the in-membrane volume of the complex identified by the phosphorescent probe (61), rotational diffusion measurements are sensitive indicators of protein-protein associations that might be critical for receptor function. Binding of hCG to the rat wild-type receptor expressed on 293 cells (LHR-wt cells) produced functional receptors which exhibited rotational correlation times longer than 1000 μsec. However, non-functional hormone-receptor complexes including wild type LH receptors occupied by deglycosylated hCG, an hCG antagonist (62), or hCG bound to LH receptors containing a substitution of arginine for lysine at amino acid 583 (LHR-K583R; (63, 64)) had significantly shorter rotational correlation times at 37°C (63 ± 8 μsec and 130 ± 12 μsec, respectively). These results suggest that functional, signaling LH receptors are present in membrane complexes that exhibit slow rotational diffusion or

are rotationally immobile. Shorter rotational correlation times for non-functional hormone-receptor complexes indicate smaller molecular weight complexes and may reflect the absence of essential interactions between these complexes and other membrane proteins.

Functional LH receptors undergo self-association

Although rotational diffusion measurements are useful for qualitative assessment of LH receptor interactions with other membrane components, they do not provide direct information on the specific interactions occurring within slowly diffusing complexes. Hormone-driven aggregation of G protein-coupled receptors like the LH receptor may be a necessary prelude to signal transduction, however, whether functional LH receptors also self-associate within slowly rotating membrane structures is not known. To determine whether hormone-occupied LH receptors self-associate into dimers or oligomers, we measured the fluorescence resonant energy transfer between fluorescein isothiocyanate (FITC)- and tetramethyl rhodamine isothiocyanate (TrITC)-derivatized LH or hCG using a method based on the reduced rate of irreversible photobleaching of FITC fluorophores when TrITC fluorophores are nearby (65). Binding of hormone to wild type LH receptors on 293 cells was accompanied by self-aggregation of luteinizing hormone receptors as indicated by values for fluorescence resonance energy transfer efficiency of 13-17%. There was little or no energy transfer between K583R-LH receptors occupied by hCG suggesting that signal transduction requires receptor-receptor interactions.

These studies support previous observations that LH receptors cluster in the plasma

membrane following hormone binding. Electron microscopy studies by Luborsky *et al.* (66) demonstrated that LH receptors associate into structures containing multiple copies of the LH receptor following exposure of rat luteal cells to high concentrations of LH. Similarly, immunofluorescence studies of the LH receptor on rat granulosa cells demonstrate the presence of large, punctate structures on the cell membrane following ligand binding (67, 68). However, because fluorescent clusters containing LH receptors visible in light microscopy or ferritin clusters in electron microscopy (66) can represent structures containing multiple copies of the receptor where the receptors are not in direct contact, fluorescence energy transfer measurements provide the first direct evidence for LH receptor association at distances of less than 100Å.

These experiments raise the question of whether signal transduction by LH receptors requires a change in receptor organization from individual receptors to aggregated receptors. To address this, we coupled the rat LH receptor to variants of green fluorescent protein (GFP) to produce an intrinsically fluorescent receptor. Using cell lines co-expressing receptors coupled to either GFP or YFP, we have shown that there is fluorescence energy transfer between LH receptors if hormone binding to the LH receptor results in cAMP formation (36) and that there is no energy transfer between non-functional mutated LH receptors following binding of LH or hCG or between functional LH receptors occupied by deglycosylated hCG (69). Thus, LH receptors that are competent to signal are in close proximity (less than 100 Å) to one another following binding of ligand. These results are consistent with studies showing dimerization of several G protein-coupled receptors including the β-adrenergic receptor (70), the δ-opioid receptor (71) and the M3 muscarinic

receptor (72) as well as rescue of non-functional β-adrenergic receptors via dimerization (70).

Desensitized LH receptors are self-associated in slowly diffusing complexes

When bound to ligand, LH receptors undergo time-dependent changes in their ability to signal while remaining within the plasma membrane. Like the β-adrenergic receptor (73), the LH receptor becomes less responsive, *i.e.* desensitized, to additional hormone stimulus within minutes after binding of hCG or LH (74, 75). The LH receptor exhibits this desensitization in response to treatment with saturating hormone concentrations, a process that has been observed *in vitro* in granulosa, luteal, and Leydig cells (75, 77-79). (76-78) In preovulatory follicles, the surge of LH which induces ovulation (79-81) also desensitizes the LH receptor. Desensitization of the LH receptor is required for initiation of oocyte meiosis (82)is followed by a decrease in cellular cAMP, despite the presence of luteinizing hormone. Once desensitized, additional hormone binding to LH receptors only minimally activates adenylyl cyclase (79) despite the fact that adenylyl cyclase is still functional and can be activated by other means (78). Desensitization of luteinizing hormone receptors following brief exposure to hormone is initially characterized by an uncoupling of the receptor from the signal transduction apparatus, rather than by a decrease in receptor number. This uncoupling process can be induced *in vitro*. After hormone binding to receptor, washing cells with a low pH buffer removes hormone from the receptor. Although the receptors are functionally undamaged by this treatment and will subsequently bind hormone (77),

desensitization has nonetheless occurred.

To determine whether the desensitized LH receptor was self-associated within large, slowly diffusing structures and whether those structures had to dissipate before the receptor could again respond to hormone, we have examined both LH receptor lateral diffusion and receptor-self association from 1-4 hrs following brief exposure of the receptor to hormone, when the receptor was desensitized but before any measurable internalization of the receptor had occurred. Lateral motions of membrane proteins diffusing without constraint from membrane components is rapid with diffusion coefficients on the order of $10^{-9}cm^2sec^{-1}$. Such unconstrained proteins also have high values for recovery of fluorescence after photobleaching of fluorescent probes. Diffusion of membrane proteins on the membranes of viable cells depends primarily and only logarithmically on the in-membrane volume of that protein. Thus, comparatively large changes in complex size are necessary to elicit a change in the rate of protein diffusion. Other protein features such as a large extracellular domain or the presence of a green fluorescent protein tag on the C-terminus of the receptor add little or no "drag" on the protein's motions. However, interactions between a fluorescently-tagged protein and other membrane proteins does significantly slow the rate of protein diffusion and can reduce the fraction of laterally mobile molecules. Thus, comparatively large changes in complex size are necessary to elicit a change in the rate of protein diffusion.

Prior to binding of ligand, rLH-GFP receptors had a diffusion coefficient of 1.6±0.3 x $10^{-9}cm^2sec^{-1}$ and a fluorescence recovery of 58±4% indicating that most receptors were laterally mobile (Figure 6, upper panel). When cells expressing LH-GFP receptors were

treated with 100 nM hCG for 30 minutes followed by removal of bound hormone by a low pH wash, there was no cAMP synthesis above basal levels in response to repeated hormone challenge for the next 4 hrs (36). For receptors desensitized by hCG treatment, fluorescence recovery decreased to less than 20% at 1 hr indicating that most receptors were laterally immobile. This response to hCG treatment was virtually identical to that of native ovine (83) and rat (84) LH receptors on luteal cells. Over the next 4 hrs there were incremental increases in both the rate of diffusion and the fraction of mobile receptors for LH receptors desensitized by LH or hCG. After 5 hrs receptors were again responsive to hormone challenge as indicated by an increase in intracellular cAMP. At this time values for diffusion coefficients and fluorescence recovery were indistinguishable from those of untreated receptors. Prior to ligand binding, there was no energy transfer between LH receptors indicating that the receptors were not self-associated (Figure 6, lower panel). However upon receptor desensitization by hCG, energy transfer efficiency increased to 18% at 1 hour. Energy transfer then decreased slowly over the next four hours. By 5 hours there was no significant energy transfer between receptors. Thus brief hormone treatment resulted in LH receptor self-association and inclusion of receptors in slowly diffusing structures. After initial signaling, receptors were non-functional and clustered in complexes that persisted in the membrane for several hours. The receptor was hormone responsive only when it is no longer self-associated and has dissociated from slowly diffusing complexes.

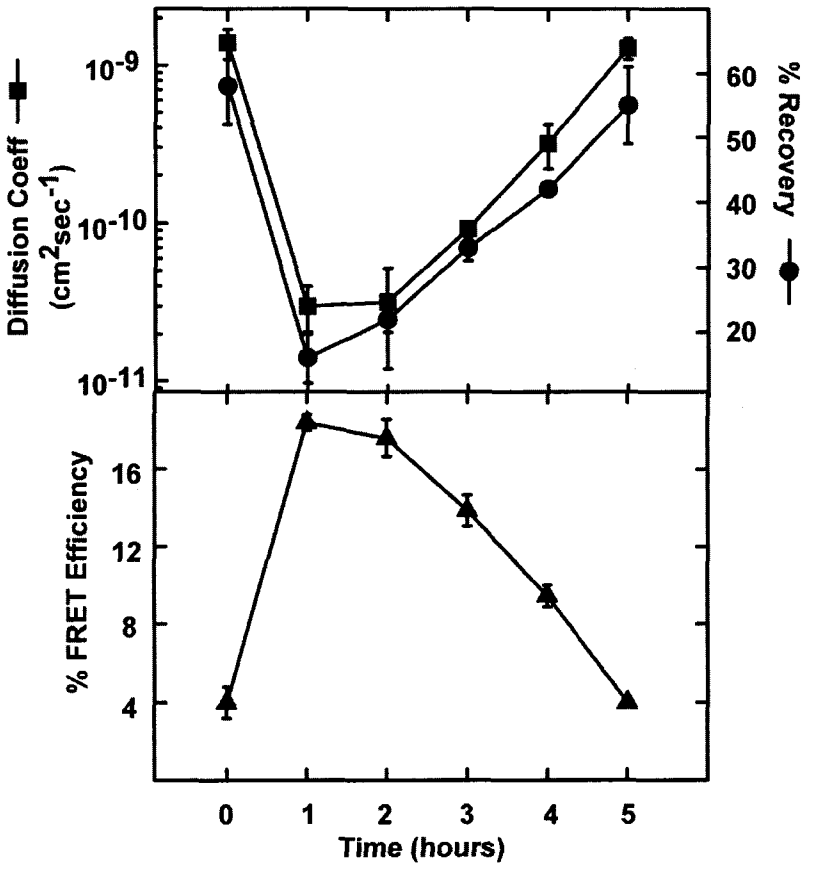

Figure 6: Spot fluorescence photobleaching recovery measurements of rLHR-GFP lateral diffusion prior to hormone binding and following hCG-induced receptor desensitization. The upper panel shows the diffusion coefficient (D) for the GFP-LHR-wt over the time course of recovery from receptor desensitization and fluorescence recovery (% recovery) of GFP-LHR-wt at the corresponding times. Receptors desensitized by either ligand exhibited significantly slower D 1 hour following desensitization. D increased over the next 4 hours until D was indistinguishable from that of untreated LHR. %Recovery decreased upon binding of hormone and then increased over time until 5 hours by which time % recovery did not differ significantly from that of untreated receptor. The lower panel show percent fluorescence resonant energy transfer efficiency (% FRET efficiency) for LH receptor fusion proteins before (0 hour) and after initiation of receptor desensitization (1-5 hrs) by 10nM hCG. At 0 and 5 hrs when receptors are hormone responsive, there is no significant energy transfer between LH receptors. When receptors were not hormone responsive there was measurable energy transfer between LH receptors. This figure was adapted from previous published results (36).

Functional LH receptors translocate into specialized membrane microdomains

Lateral diffusion studies of GFP-LH-wt receptors suggested that most unoccupied LH receptor were laterally mobile with a fast rate of lateral diffusion and that binding of ligand slowed receptor lateral diffusion 6-10 fold and reduced the fraction of mobile receptors (85). The dramatic slowing of receptor lateral diffusion and a reduction in the fraction of mobile receptors are consistent with receptor trapping in rafts following ligand binding. It has been suggested that rafts may serve as signaling platforms in the plasma membrane. A number of plasma membrane receptors including the IgA receptor (86), epidermal growth factor (EGF) receptor (87), and the tumor necrosis factor (TNF) receptor (86) move into membrane rafts during signal transduction. Translocation of membrane proteins into rafts can be driven by receptor crosslinking in the absence of ligand. Fcα receptors, upon crosslinking, move into rafts containing tyrosine kinases and are phosphorylated (88).

To test whether the LH receptor partitions into membrane rafts following binding of ligand, we stably expressed a FLAG-tagged rat LH receptor in CHO cells using a FLAG-rLH receptor vector kindly provided by Dr. K.J. Menon from the University of Michigan. Stable expression of the FLAG-rLH-wt receptor made it possible to identify the LH receptor on Western blots in the unbound and bound state. hCG-treated FLAG-rLH receptors were consistently located in 25-40% sucrose (Figure 7) together with caveolin, a protein which serves as a lipid raft membrane marker. Unoccupied LH receptors were found in a high density lipid membrane and were not colocalized with caveolin (data not shown). The

appearance of LH receptors within rafts following binding of hormone are consistent with imaging of the wild type LH receptor coupled to GFP. The unoccupied GFP-coupled LH receptor had very diffuse distribution in the plasma membrane and underwent striking redistribution into punctate fluorescent clusters on the membrane shortly after being exposed to hormone (85). Whether the preferential localization of plasma membrane proteins such as LH receptors into discrete domains in which molecular motions are restricted has functional significance in, for example, receptor desensitization, as is shown in our working model for LH receptor localization in the membrane (Figure 8), remains an unanswered question.

Conclusions

These studies underscore the dynamic nature of the LH receptor's interactions within the plasma membrane, summarized in our working model (shown in Figure 8), both in response to binding of ligand, signaling, and subsequent receptor desensitization. They also raise a number of questions about the receptor and its interactions. Presumably, if rafts serve as signaling platforms, there are time-dependent interactions between the receptor and proteins that transduce hormone signal or desensitize the receptor to prevent further activation of adenylyl cyclase. Whether these various proteins are available within rafts or move into or out of the raft environment in some orchestrated fashion is an intriguing question.

Self-association of the receptor is also a potentially interesting phenomena from

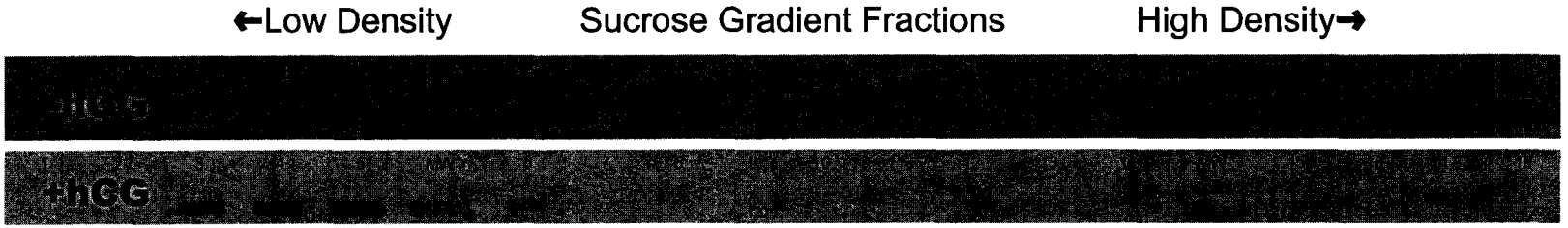

Figure 7: Western blots of FLAG-rLH-wt receptor from CHO cells appearing in various sucrose density fractions after isopycnic centrifugation. The upper photograph shows receptors from untreated CHO cells appearing in fractions 13-15 (approximately 50-65% sucrose). The lower photograph shows receptors from hCG-treated CHO cells which consistently appeared in fractions 3-6 (12-25% sucrose) together with caveolin (data not shown).

several points of view. On a molecular level, the association of LH receptors may require both appropriate receptor conformation as well as specific dimerization sequences on both receptors. There has been such a sequence proposed for the β-adrenergic receptor (89) but this sequence is not contained within the transmembrane domains of the rat LH receptor and does not appear to be generally well conserved among G protein-coupled receptors (90). Guo and coworkers have proposed that the fourth transmembrane domain of the dopamine D2 receptor may contain sites used in formation of D2 receptor homodimers.

Other questions of interest include the relationships between receptor aggregation and signaling and desensitization as well as membrane localization of receptors during receptor internalization. We show in Figure 8 that desensitized receptor, presumably following binding of β-arrestin, are present in large molecular weight structures which we hypothesize are localized in membrane rafts. This is based on a study in collaboration with Dr. Mary Hunzicker-Dunn at Northwestern University which shows that LH receptors from porcine granulosa cells are present in large, slowly rotating complexes *only* when LH receptors are desensitized (91). Treatment of membranes with antibodies to β-arrestin blocks LH receptor desensitization and results in receptor-containing complexes that are smaller and have fast rotational correlation times. For LH receptors, these temporal events as well as the membrane sites involved in receptor binding to ligand, signaling via G proteins, receptor interaction with arrestins, and subsequent internalization are still being actively studied. Lastly, the time-dependent increase in lateral diffusion of the desensitized LH receptor together with a decrease in the extent of receptor self-association are indicative of large complexes that slowly dissociate until free receptor is again available for interaction with

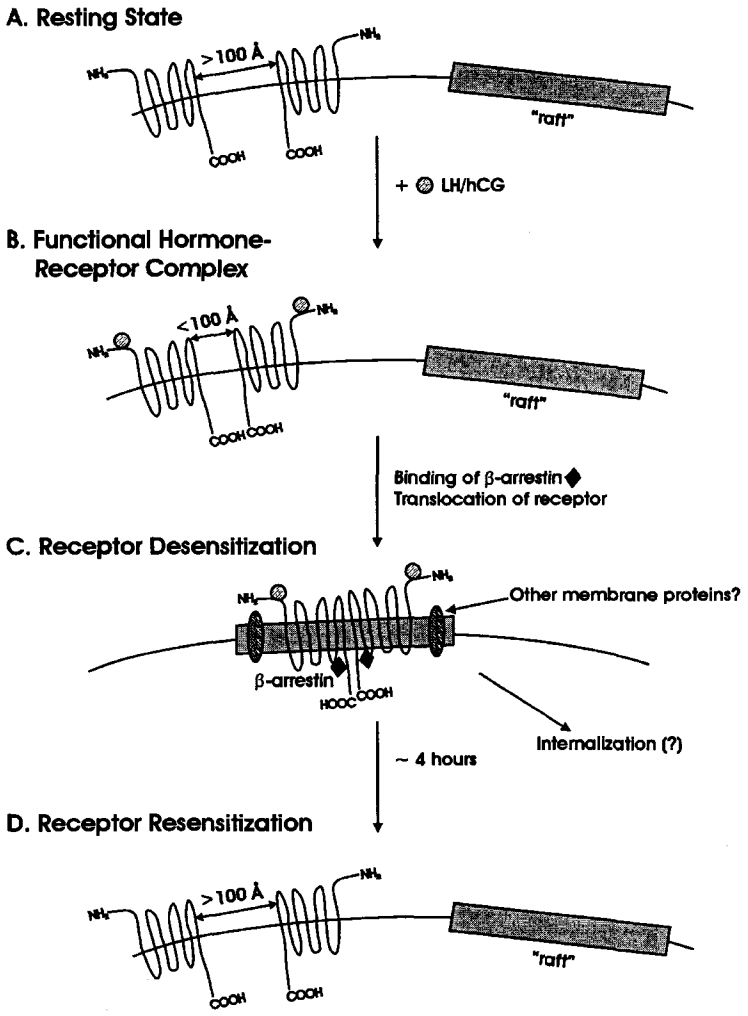

Figure 8: We have developed a working model for LH receptor interactions following hormone binding as well as during desensitization and resensitization of the receptor based on the physical evidence described in this review. Resting LH receptors (shown in panel A), located in the bulk plasma membrane rather than in membrane rafts, exhibit fast lateral diffusion and do not appear to be self associated until they have bound hormone agonists (panel B). Binding of hormone also drives receptors into plasma membrane rafts. Whether the receptor translocates into these structures as receptor monomers or dimers is not known. Desensitization of the receptor in response to β-arrestin binding (panel C) is associated with slow rotational diffusion of the receptor, presumably as a result of incorporation of LH receptors into large molecular weight complexes which may be located in rafts. Resensitization of the receptor (panel D) is characterized by a reduction in receptor-receptor interactions and by fast rates of receptor lateral diffusion.

ligand. Whether these complexes dissociate within specific membrane microdomains or move out of membrane rafts prior to dissociation is also not known. Biophysical methods, particularly those applicable to examining receptors on viable cells, will be valuable tools for resolving these questions.

ACKNOWLEDGMENTS

We would like to acknowledge the contributions made by past and present members of Dr. Roess' research group, Ying Lei, Dr. Regina Horvat, Dr. Mary Cahill, Guy Hagen, and Dr. Cynthia J. Brady as well as Drs. Mary Hunzicker-Dunn and George Barisas who have provided invaluable collaborative assistance. We would also like to thank the Endocrine Society for permission to use the data shown in Figure 6. This data was originally contained in "Luteinizing receptors are self-associated in slowly diffusing complexes during receptor desensitization" by Horvat, R.D., Barisas, B.G. and Roess, D.A. and published in *Molecular Endocrinology*, volume 15(4), pages 534-542 (2001).

CHAPTER 3[2]

Luteinizing Hormone Receptors Translocate to Plasma Membrane Microdomains Following Binding of Human Chorionic Gonadotropin[2]

ABSTRACT

Receptor-mediated signal transduction by G protein-coupled receptors can involve redistribution of plasma membrane receptors into membrane structures that are characterized by insolubility in Triton X-100 and low buoyant density in sucrose gradients. Here we describe the translocation of wild type rat luteinizing hormone receptors from the bulk membrane into membrane microdomains (rafts) following the binding of hCG. In sucrose gradient ultracentrifugation of plasma membranes from cells stably expressing FLAG-tagged LHR-wt, receptors were located in high density membrane fractions before binding of hormone and in low density fractions following hCG treatment. Receptor translocation to low density sucrose fractions did not occur when cells were pretreated with 1% MβCD which reduces membrane cholesterol and disrupts rafts. Single-particle tracking of individual FLAG-LHR-wt receptors showed that hCG-treated receptors become confined in small compartments with a diameter of 86 ± 36 nm, which is significantly smaller than the regions

---

2

This chapter was adapted from Steven M. L. Smith, Yin Lei, Jingjing Liu, George Barisas and Deborah A. Roess (2006) Luteinizing hormone receptors translocate to plasma membrane microdomains following binding of human chorionic gonadotropin, *Endocrinology*, in press.

accessed by the untreated receptor (230 ± 79 nm). After disruption of rafts by MβCD, receptors were no longer confined in these small compartments which also decreased levels of cAMP production in response to hCG. Finally, translocation of LH receptors into rafts required a functional hormone-receptor complex, but did not occur after extensive receptor crosslinking which elevated cAMP levels. Thus, retention of LHR in rafts or small membrane compartments is a characteristic of functional, hormone-occupied LHR-wt. Although raft translocation was not essential for cAMP production, it may be necessary for optimizing hormone-mediated signaling.

INTRODUCTION

Several lines of evidence suggest that functional LHRs are clustered within relatively large structures following the binding of hormone. Electron micrographs of LHR on rat granulosa cells show large clusters of receptors that form only after binding of hormone (66) Immunofluorescent labeling of rat LH receptors shows similar responses in granulosa cells (67). Wild type rat LH receptors tagged with green fluorescent protein (LHR-GFP) aggregated within minutes following receptor binding of either LH or hCG on viable cells (85). This aggregation was accompanied by close interactions between individual receptors, as described previously by other strategies for evaluating fluorescence resonance energy transfer between LH receptors (92), and indicated by comparatively high values for fluorescence energy transfer efficiency between receptors tagged with variants of green fluorescent protein (36). The presence of receptors in relatively large structures has also been suggested by lateral diffusion studies of the LH receptor in luteal cells from sheep (83) and rat (84) in which most LH receptors were laterally immobile.

Clustering of the rat LH receptor involves the movement of diffusely distributed receptors into discrete membrane sites (36). One question raised by such observations is whether the receptors cluster at arbitrary sites on the plasma membrane or become confined in membrane microdomains. Membrane microdomains include so-called rafts which, because of their high cholesterol and sphingolipid content, "float" in sucrose gradients. Rafts are enriched, not only with sphingolipids and cholesterol (3), but with GPI-anchored proteins (93). The lateral diffusion of specific membrane proteins within these microdomains is also

reduced (94). Membrane domains, which on some cells may comprise a substantial fraction of the plasma membrane (18, 95), can contain membrane proteins necessary for cell signaling such as G proteins (96) and adenylyl cyclase (97). There is also evidence for transient protein targeting to membrane rafts including proteins involved in the regulation of G protein signaling (98). Together, these observations have led to suggestions that rafts might serve as signaling platforms for G protein-coupled receptors. We believe LHR signaling may be accomplished by targeting the receptors to environments that favor receptor-receptor interactions and G protein-mediated signaling.

An additional question raised by these observations is whether LHR function is dependent on receptor translocation into rafts. There are physical differences between functional hormone-receptor complexes, i.e., hCG- and LH-occupied wild type LH receptors, and those complexes that do not activate adenylyl cyclase. As examples, binding of the hCG antagonist deglycosylated hCG (62) to rat LHR does not produce receptor self-association (69) or slow receptor rotational diffusion to the same extent observed for hCG-occupied LHR (99). These results indicate that larger receptor-containing structures do not form after receptor binding of deglycosylated hCG. Similarly, there is no self-association of rat LH receptors containing a substitution of arginine for lysine at amino acid 583 (LHR-K583R) which either partially (63) or fully (64) eliminates the cAMP response to hCG. Thus, if rafts serve as signaling platforms for rat LH receptors, non-functional receptors may be excluded in some manner from these structures or, alternatively, lack some critical receptor feature needed to direct the hormone-occupied receptor to rafts.

To address these questions, we have isolated membrane fragments from hCG- or

deglycosylated hCG-treated CHO cells expressing wild type rat LH receptors and from hCG-treated LHR-K583R which have been all been labeled at their N-terminus with the FLAG sequence. To further demonstrate the localization of functional LH receptors within rafts, we have treated cells with MβCD which can efficiently remove cholesterol from the plasma membranes of live cells (100, 101) and thus disrupt raft structure. To independently examine the effects of hCG on LH receptor motions within the plasma membrane, we have used single-particle tracking methods to evaluate the size of membrane compartments accessed by individual receptors as visualized microscopically on viable cells (59). Finally, we examined whether disruption of membrane rafts is accompanied by altered signaling in CHO cells in response to hCG (69)

MATERIALS AND METHODS

Materials

Dulbecco's modified Eagle's medium (DMEM) containing 4.5 g/L glucose was purchased from VWR (West Chester, PA). Geneticin was purchased from Invitrogen (Carlsbad, CA). MβCD, HEPES and non-essential amino acids were purchased from Sigma-Aldrich (St. Louis, MO). Fetal bovine serum (FBS) was purchased from Gemini Bio Products (Woodland, CA). hCG was purchased from Research Diagnostics Inc. (Flanders, NJ). Cellular cAMP was measured using a "Direct Cyclic AMP Correlate-EIA" kit (Assay Designs, Ann Arbor, MI) as per the Manufacturers instructions. Colloidal gold (40 nm) was purchased from Ted Pella, Inc. (Redding, CA). Deglycosylated hCG was a kind gift from Dr. Henry Keutman.

Cell lines

To test whether the rat wild type LH receptor becomes associated with membrane rafts following binding of ligand, we generated a stable cell line expressing the FLAG-tagged receptor. Dr. K.J. Menon from the University of Michigan kindly provided us with N-terminal FLAG- tagged LHR subcloned into the pFLAG vector (Sigma, St. Louis, MO). Using the FLAG-LHR vector we made a mutation of lysine 583 to arginine (FLAG-LHR-K583R). CHO cells were stably transfected with 5 μg of the FLAG-LHR or K583R-FLAG-

LHR vector using Lipofectamine-Plus (Gibco-BRL, Gaithersburg, MD) as per Manufacturers instructions. Selection of stable clones expressing the FLAG-tagged receptors was based on the acquisition of geneticin (G418) resistance. CHO cell lines were maintained in Dulbecco's modified Eagle media supplemented with 4.5 g/mL glucose and containing 10% FBS, 100U/mL penicillin, 100 μg/mL streptomycin and 1x MEM non-essential amino acids (Sigma Chemical Co., St.Louis, MO) that was supplemented with 400μg/mL G418.

Isolation of plasma membrane rafts

Cells were incubated with either 100nM hCG or 100 nM deglycosylated hCG (62), or PBS for 1 hour at 37°C prior to cell lysis. To isolate membrane rafts from LHR-wt and LHR-K583R cells, 5 x 10^7 cells were washed two times with phosphate-buffered saline, pH 7.2 (PBS) and lysed for 5-10 minutes on ice in 1ml of a buffer containing 25mM MES, 150mM NaCl, 2mM EDTA, 20% glycerol, 0.25% Triton-X100, and protease inhibitors including aprotinin, leupeptin, EDTA, and PMSF (Roche). A low speed 300 x g spin was used to remove cell nuclei and large cell debris. For raft studies, 1 mL of this supernatant containing plasma membrane fragments was then combined with 1mL of 80% sucrose containing 0.25% Triton-X100 and protease inhibitors to produce a 40% sucrose solution. A discontinuous sucrose gradient from 10-80% was created with the sample in 40% sucrose layered within this gradient. The gradient was loaded into a Beckman SW-41 swinging bucket rotor and spun at 175,000x g for 20 hours at 4°C. After the spin, eighteen 650μL fractions were carefully collected from the top of the gradient downward. A 50 μL aliquot

from each fraction was diluted 1:1 with 95% SDS and 5% β-mercaptoethanol. After separation of proteins from each fraction using SDS-PAGE and transfer of proteins to nitrocellulose, the LH receptor was identified using 30μg of an anti-FLAG M2 monoclonal antibody (Sigma, St. Louis, MO). The amount of receptor in each fraction was measured using a Bio-Rad GS-800 calibrated densitometer. The sucrose concentration in each fraction was determined using a Bausch and Lomb refractometer. In some experiments, cells were pretreated for 1 hr at 37°C with 1% methyl-β-cyclodextrin (MβCD) in serum-free Dulbecco's modified Eagle medium containing high glucose prior to incubation with hCG or PBS or with 100 nM anti-FLAG antibody for 45 min at room temperature followed by a second 45 min incubation with 1 μM anti-mouse IgG (Sigma). MβCD neither binds nor inserts in the plasma membrane of cells but rather extracts cholesterol by including it in a central non-polar cavity of cyclic oligomers of glucopryanoside in α-1,4-glycosidic linkages (93). At this concentration, it was non-toxic to cells and did not compromise cell integrity (data not shown) (52).

Single-particle tracking of FLAG-LHR-wt receptors on individual cells.

Lateral dynamics and the size of domains accessed by individual FLAG-LHR-wt were evaluated using single-particle tracking methods as described by Kusumi et al. (59). Probe was prepared using 40 nm nanogold particles conjugated with the lowest possible concentration of anti-FLAG monoclonal antibody (mAb) needed to stabilize the gold solution. This gold-labeled antibody was then incubated with CHO cells expressing FLAG-

LHR-wt receptors. The anti-FLAG-gold concentration, typically 15 μg/mL, was then further reduced by addition of 1% BSA in PBS until there were approximately 1-4 gold particles per cell. Probe binding was specific for FLAG-tagged receptors; when cells were preincubated with a 10-fold excess of anti-FLAG antibody, no anti-FLAG-gold particles were detected on cells. In some experiments, cells were treated with 100 nM hCG for 1 hr after labeling receptors with anti-FLAG mAb or cells were pre-treated with 1% MβCD for 1 hr prior to labeling with anti-FLAG antibody.

Individual nanoparticles were imaged using differential interference contrast with a 1.4 N.A. 63x objective in a Zeiss Axiovert 135 microscope. Images were acquired using a Dage IFG-300 camera and were recorded for 2 min (3600 frames) at approximately 30 nm/pixel under the control of Metamorph software from Universal Imaging (Downingtown, PA). The trajectories for individual gold particles were segmented into domains by calculation of statistical variance in particle position over times using procedures developed previously(102-104). The variance of a particle's position was calculated within windows of varying duration. These windows were translated along the particle trajectory, producing a variance plot that exhibits peaks that indicate inter-domain boundaries. These results were analyzed to yield the domain size and residence time for each particle. Effective macroscopic diffusion constants were calculated as the square of the domain diagonal divided by four times the residence time in the domain as previously described (104).

RESULTS

Functional, but not non-functional, LH receptors appear in membrane rafts following hCG binding.

After isopycnic centrifugation of plasma membrane fractions from CHO cells expressing FLAG-LHR-wt, unoccupied LH receptors were found in sucrose fractions of relatively high densities (Figure 9). Immunoblots of FLAG-LHR-wt receptors identified by anti-FLAG antibody were developed as previously shown (105) and the relative amount FLAG-LHR-wt in each sucrose fraction was quantified using densitometry. Over 90% of FLAG-LHR-wt receptors were localized in sucrose fractions 10-15 where sucrose concentrations ranged from approximately 36-56%. Following treatment of cells with 100 nM hCG, there was marked change in the distribution of receptors to the lower density sucrose fractions. Over 80% of hCG-treated FLAG-LHR-wt receptors consistently appeared in fractions 3-7 which contained 14-26% sucrose. In addition, over 90% of the hormone-bound receptors appeared in these less dense sucrose fractions than did the untreated receptors.

The translocation of LH receptors from high to low density membrane fractions required functional hormone-receptor complexes; LHR from CHO cells expressing FLAG-LHR-K583R treated with hCG or FLAG-LHR-wt cells treated with deglycosylated hCG remained associated with higher density sucrose fractions (Figure 10) despite the presence of bound ligand. Crosslinking of FLAG-LHR-wt receptors using an anti-FLAG antibody

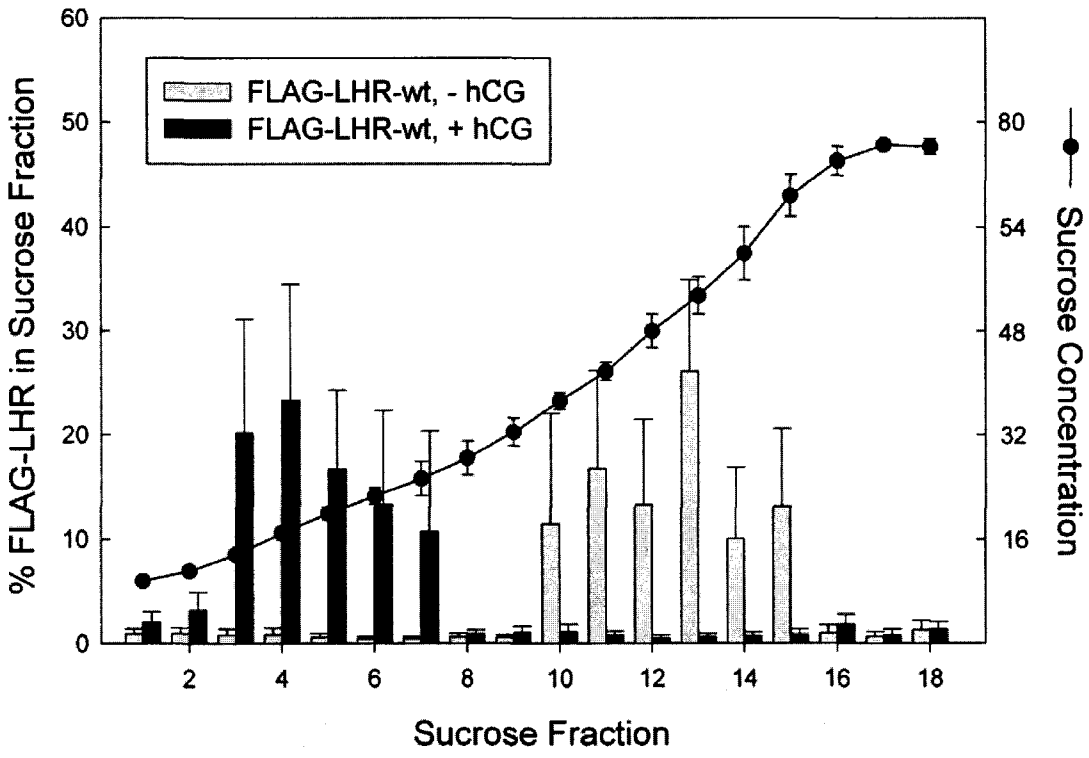

Figure 9: Before exposure to hCG, wild type rat LH receptors appear in high density fractions of the sucrose gradient. After treatment of CHO cells with 100 nM hCG, receptors appear in lower density fractions. Membrane fractions were separated as described in Materials and Methods and densitometry was used to estimate the relative amount of LH receptor contained in each fraction. Results shown are the mean and standard error of the mean (S.E.M.) for at least 5 individual experiments. The sucrose concentration in each fraction was evaluated in five separate experiments using a Baush and Lomb refractometer together with a standard curve. Because, for any given fraction, the sucrose concentration did not vary appreciably from experiment to experiment, the average sucrose concentration for five representative experiments is shown.

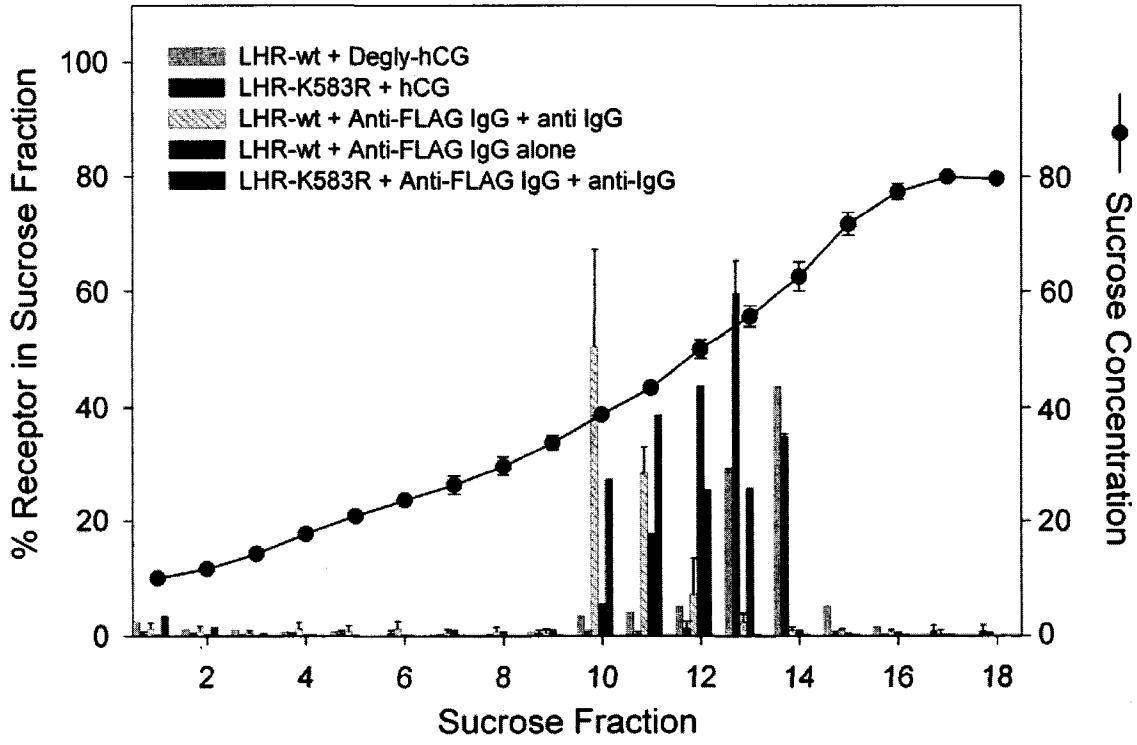

Figure 10: Translocation of LH receptors into buoyant membrane fractions required functional LH receptors. Neither wild type rat LH receptors treated with 100 nM deglycosylated hCG, LHR-K583R treated with hCG or antibody treated (anti-FLAG antibody alone) or extensively crosslinked LHR-wt (anti-FLAG antibody followed by excess anti-mouse IgG) were found in plasma membrane rafts.

either alone or together with an excess of a secondary polyclonal anti-mouse antibody (Figure 10) had no significant effect on the distribution of FLAG-LHR-wt within the sucrose gradient.

Depleting membrane cholesterol disrupts membrane rafts and decreases cAMP signals in response to hCG treatment.

Preincubation of cells for 30 minutes with 1% MβCD disrupted membrane rafts containing the LH receptor. Over 93% of hCG-treated FLAG-LHR-wt were found in fractions 10-12 following exposure of cells to 1% MβMD (Figure 11) which was essentially unchanged from the distribution of unoccupied FLAG-LHR-wt receptors on CHO cells treated with MβCD (data not shown) and to the distribution of unoccupied receptors shown in Figure 9. Interestingly, disruption of LHR-containing rafts with MβCD did not affect caveolae. Western blots prepared in tandem with those used to identify FLAG-LHR-wt were probed with an anti-caveolin antibody from Santa Cruz Biotechnology. Caveolin remained broadly distributed in lower density sucrose fractions under all experimental conditions (Figure 11) suggesting that LH receptors are associated with membrane microdomains that are distinct from caveolin-containing membrane regions.

Disruption of membrane rafts also reduced cell signaling in response to hormone. It has been suggested that plasma membrane rafts may serve as signaling platforms, effectively concentrating receptors and other plasma membrane molecules necessary for initiating down-stream signaling events. If this were correct, disruption of membrane rafts

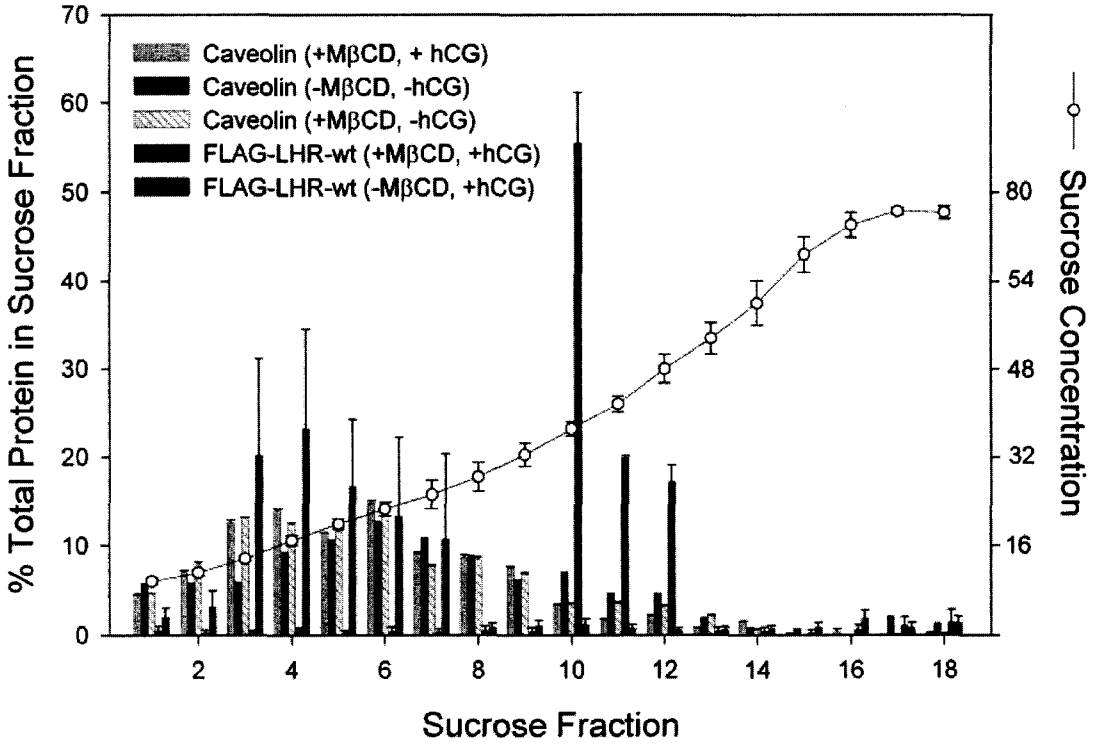

Figure 11: Disruption of plasma membrane rafts by extraction of cholesterol from the plasma membrane eliminated translocation of FLAG-LHR-wt into low density sucrose fractions. Results shown are the mean and S.E.M. for two separate experiments. In addition, anti-caveolin-1 antibody was used to identify caveolin in sucrose fractions. The distribution of caveolin in fractions 1-10 remained relatively constant in untreated cell samples and in samples exposed to hCG or MβCD.

should reduce or eliminate selective signaling events dependent on this membrane micro-environment. We examined accumulation of cAMP in response to hCG in cells pretreated with 1% MβCD. Although, in our hands, changes in cAMP levels in CHO cells were modest, typically 2 to 7-fold over basal levels, pretreatment of cells with MβCD, nonetheless reduced hCG-mediated increases in intracellular cAMP to basal levels (Figure 12). Interestingly, extensive crosslinking of LHR-wt caused a significant increase in cAMP production to levels comparable to those of hCG-treated CHO cells or cells treated with forskolin even though this antibody-induced form of receptor self association was not sufficient to drive receptor translocation from the bulk membrane to rafts (Figure 10).

Single-particle tracking of hCG-occupied FLAG-LHR-wt receptors demonstrates "trapping" of receptors in small membrane compartments.

Figure 13 shows a representative particle track for an untreated LH receptor and for an hCG-treated receptor. The single-particle tracking results demonstrate that a gold particle bound to FLAG-LHR-wt exhibits distinctive motions in the presence and absence of hCG. hCG treatment reduces the size of compartments containing FLAG-LHR-wt from 230 ± 79 to 86 ± 36 nm (Table 1). Although the average residence time for receptors within microdomains and the number of microdomains, 6 ± 2 and 5 ± 2, accessed by the receptor in two minutes did not differ significantly for untreated and hCG-treated cells, respectively, an individual receptor's rate of diffusion (D) within each domain was reduced by a factor of ten following hCG treatment. Figure 14 illustrates these results for untreated and hCG-

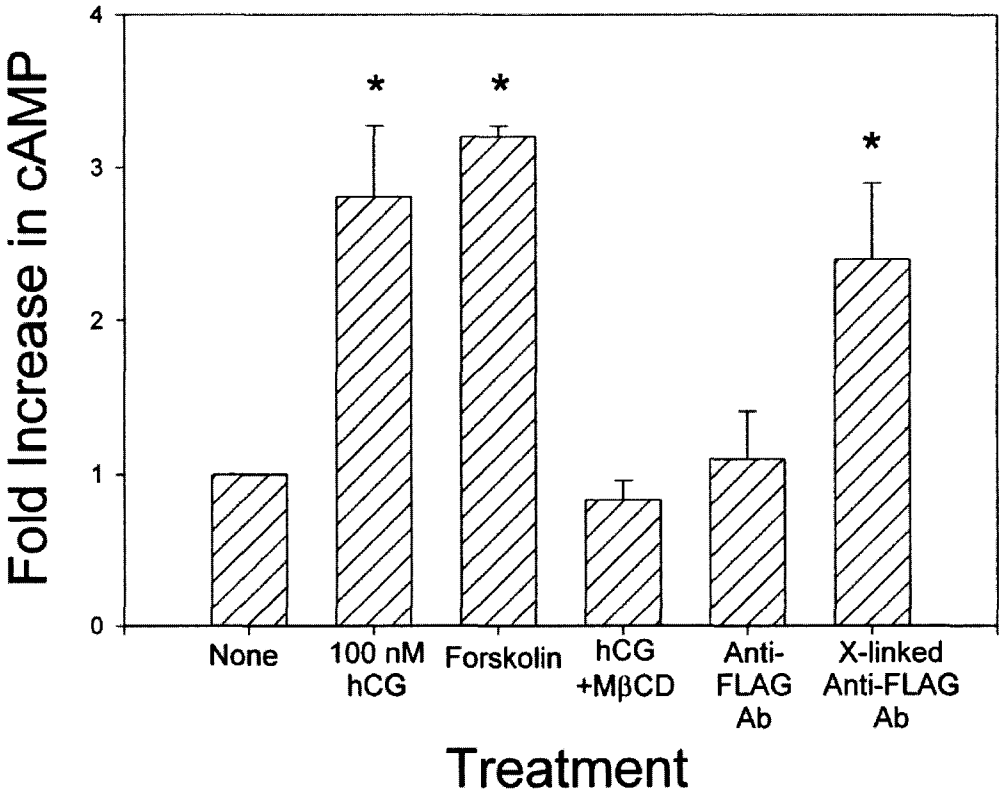

Figure 12: cAMP levels were assayed in CHO cells using a colorimetric cAMP kit from Assay Designs. There was an approximately 3-fold increase in cAMP in response to cell treatment with either 100nM hCG or forskolin. 1% MβCD reduced cAMP levels in hCG-treated samples to basal levels. Although exposure of FLAG-LHR-wt to monoclonal anti-FLAG antibody had no effect on cAMP levels, crosslinking of the receptor with an excess of anti-mouse IgG elevated cAMP levels to values comparable to those of hCG-treated cells. Results are the mean and S.E.M. for at least 5 experiments performed in triplicate.

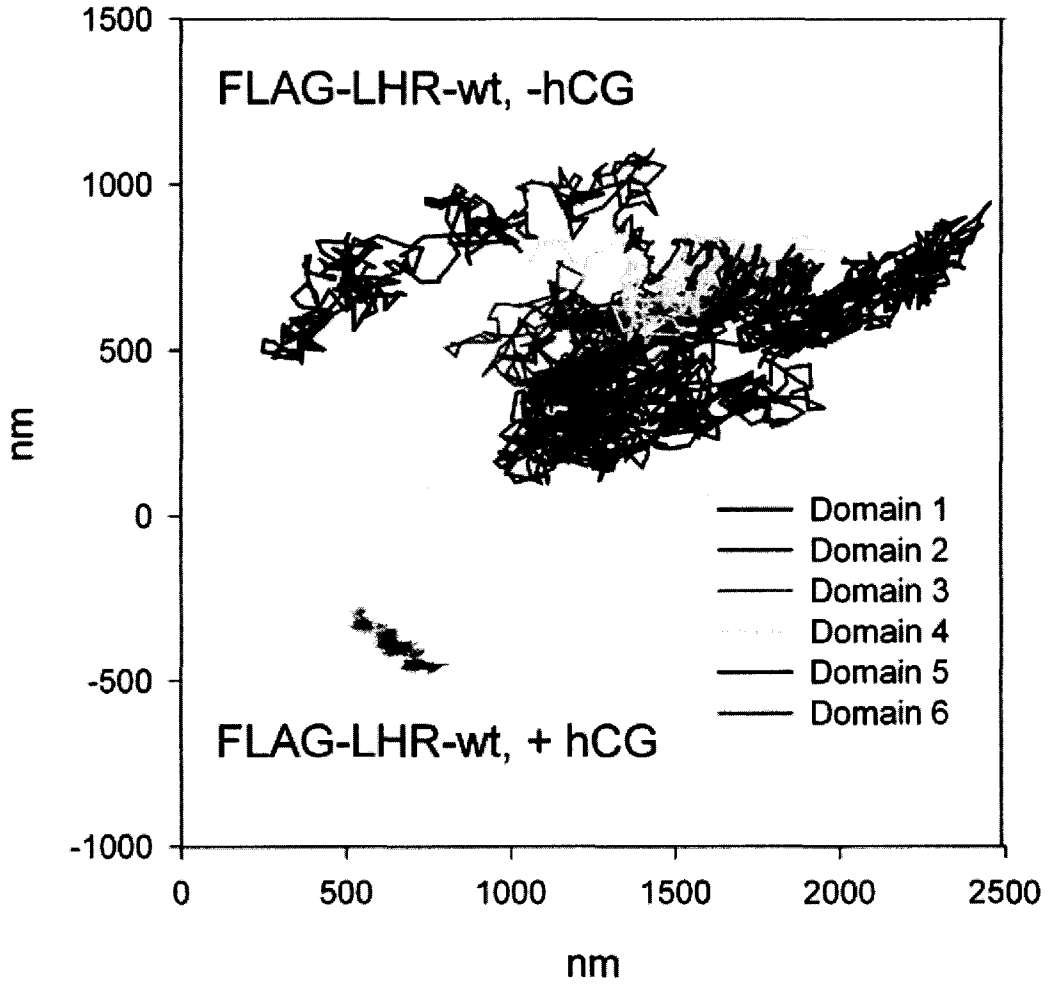

Figure 13: Representative trajectories for a single FLAG-LHR-wt receptor on an untreated cell or a cell treated with hCG. Each track represents data obtained during a single experiment of approximately 2 minutes. The representative track for untreated FLAG-LHR-wt cells shows receptor confinement within five compartments while the representative track for hCG-treated cells shows confinement within three compartments. Individual compartments within a given particle trajectory were identified as described in Materials and Methods.

treated cells and shows that as receptors access progressively larger membrane microdomains, their rate of diffusion within those microdomains increases.

Because MβCD pre-treatment largely reversed the effects of hCG on compartment size and receptor lateral diffusion, it seems plausible that compartments retaining hCG-treated receptors are rafts. As shown in Table 1 and illustrated in Figure 13, MβCD pre-treatment results in a significant increase in the size of membrane compartments containing LHR-wt. The size of these compartments does not differ significantly from those accessed by untreated FLAG-LHR-wt receptors and, together with results from sucrose density gradient centrifugation experiments, suggests that these unbound receptors are residing in the bulk membrane rather than rafts.

Finally, we evaluated single-particle tracks for non-functional hormone-receptor complexes. As shown in Figure 14, FLAG-LHR-wt receptors treated with deglycosylated hCG as well as FLAG-LHR-K583R receptors treated with hCG remained in large membrane compartments where they exhibited comparatively fast lateral motions. These results were consistent with previous studies of LH receptor rotational dynamics which suggest that receptors within non-functional hormone-receptor complexes exhibit comparatively short rotational correlation times suggesting that they are located within smaller complexes (99).

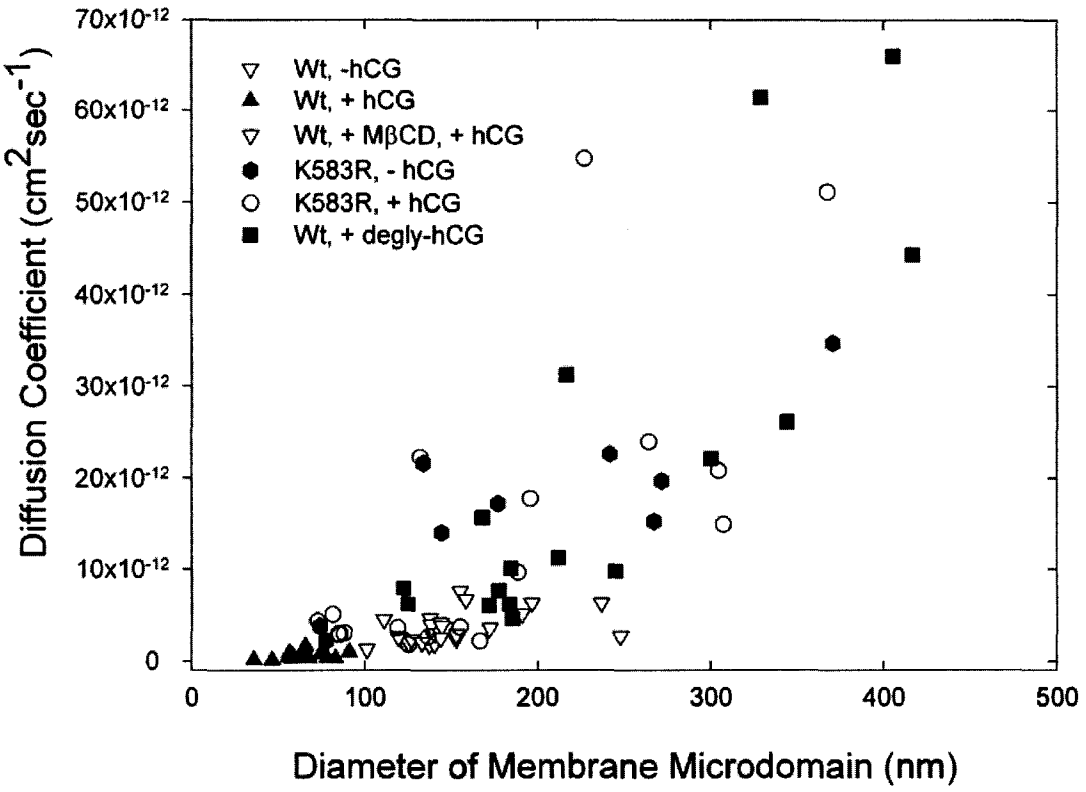

Figure 14: Single particle tracking of individual FLAG-LHR-wt receptors labeled with gold-conjugated anti-FLAG antibody. The compartment size and diffusion coefficient for the LH receptor within that compartment were calculated as described in Methods and Materials. Results shown are from individual cells that were untreated (△), treated with hCG after labeling of receptors with gold-conjugated anti-FLAG antibody (■) or were pretreated with 1% MβCD prior to labeling with anti-FLAG antibody and treatment with hCG (▾). Data presented in this figure for each conditions are from cells examined in separate experiments on three different days.

DISCUSSION

Our results demonstrate that wild type LHRs, if occupied by a functional ligand, are capable of moving from the bulk membrane into small nm-diameter plasma membrane compartments with characteristics of lipid rafts. The translocation of LHR to low density membrane regions appears to be characteristic of the functional hormone-receptor complex and is not observed when either the LHR is non-functional or when a hormone antagonist has bound to the wild type receptor. Moreover, the regions within which hormone-treated LHR-wt receptors are confined are small. Translocation of receptors into rafts is also implicated in receptor-mediated signaling as demonstrated by the decrease in hCG-mediated cellular levels of cAMP when rafts were disrupted. The appearance of receptors within low density, detergent-insoluble membrane fractions occurs upon binding of hormone agonist to LHR. This is similar to results of Bramley and Ryan (106) who separated membrane fragments from homogenated ovaries of superovulated ewes on continuous sucrose gradients. They isolated two distinct membrane fractions that displayed hCG binding and, as a result, suggested that there might be two populations of LH receptors present on granulosa cells. They also characterized selected proteins in "heavy" and "light" membrane fractions containing LHR including adenylyl cyclase which, interestingly, associated with the "heavy" receptor population.

The mechanism involved in targeting of LHR to rafts is not clear. Proteins found in plasma membrane rafts include transmembrane proteins with attached lipid groups including, most commonly, GPI or palmitate (107). There is evidence for palmitoylation of the LH

receptor at two cysteines located in the receptor's intracellular carboxy terminal (108). Although mutations to the palmitoylated cysteines did not affect cAMP production, the mutated receptors were internalized more quickly than wild type receptors, apparently through an arrestin-mediated pathway (109). Point mutations to palmitoylation sites on the LH receptor C terminus also eliminates LHR-wt translocation into rafts (110). However, it is not known whether there is reversible palmitoylation of the wild type LHR or whether the binding of ligand alters equilibrium between palmitolylated and non-palmitoylated LH receptors. This appears to be the case for β-adrenergic receptors, G protein-coupled receptors structurally related to LHR, which undergo palmitoylation/depalmitoylation cycling with binding of agonist favoring receptor depalmitoylation (111). If palmitoylation were necessary for targeting of a ligand-activated G protein-coupled receptor to rafts, depalmitoylation would be predicted to reduce the likelihood of finding, for example, β-adrenergic receptors in rafts. However, the role for palmitoylation in receptor-mediated signaling (112) and raft localization is generally unclear and may prove ultimately to be receptor-specific.

Receptor aggregation, either together with receptor palmitoylation or independently, may increase the affinity of the LH receptor for rafts. Signaling by multi-chain receptors such as T-cell and B-cell antigen receptors are present in the bulk membrane prior to crosslinking by multivalent antigens (113, 114). Crosslinking may shift the equilibrium distribution for membrane proteins within the lipid bilayer and favor interactions between proteins and more ordered lipid microdomains such as rafts as has been demonstrated for lipid-anchored proteins within artificial lipid monolayers (14). In our hands, LH receptor

self-association (69) as well as raft localization are characteristic of functional hormone-receptor complexes. One could hypothesize that agonist-induced associations between LH receptors causes translocation of receptors to rafts. Interestingly however, presumably random interactions between LHR receptors following antibody crosslinking, are not sufficient to drive receptor translocation to rafts but are sufficient for activation of adenylyl cyclase in the absence of hCG. Although targeting of proteins to rafts can be initiated by antibody crosslinking of, for example, T-cell and B-cell antigen receptors (113, 114) and the Type I Fcε receptor on rat basophilic leukemia cells (115), this was not the case for antibody-crosslinked LH receptors, suggesting that LH receptors required binding of a hormone agonist and potentially specific receptor conformations for targeting of activated receptors to rafts.

It appears that membrane rafts may serve as a signaling platforms for the LH receptor although the specific signaling event(s) are uncertain. Spatial coordination of key signaling proteins in lipid rafts may provide a rapid, efficient and specific mechanism for promoting signal transduction from extracellular to intracellular mechanisms while also preventing cross-talk between pathways (13, 116). As an example, Type I Fcε receptors form, at a minimum, receptor dimers that are tyrosine phosphorylated by Lyn and then colocalize with Lyn in membrane rafts (115). Other downstream signaling molecules also appear within rafts. Oh and Schnitzer have shown that G_i and G_s are targeted to, and concentrated in, lipid rafts (13) and some isoforms of adenylyl cyclase are associated with these membrane structures (117-119). If rafts serve to concentrate these proteins, cholesterol depletion and raft disruption may disperse raft-associated proteins and reduce the likelihood of protein-

protein interactions necessary for cell signaling. Indeed, MβCD treatment reduced FRET between GPI-anchored proteins (120) and signal transduction by these proteins (121). Other studies have shown that cholesterol is important for lipid raft formation and that its depletion decreases signal transduction efficiency (52, 122).

Single-particle tracking studies provide some insight into the nature of LH receptor-containing structures. Upon binding ligand, the LHR-wt becomes largely confined within small compartments with an average diameter of 86 nm. For the most part, the receptor remains within these regions for comparatively long times and appear to diffuse pseudo-randomly before being captured within another compartment of similar size. Similar behavior has been described and analyzed by Kusumi and coworkers (102) for selected phospholipids and for transferrin receptor (123) and by Daumas et al. (103) for the μ opioid receptor, a G protein-coupled receptor involved in pain responses. Daumas argues that μ opioid receptor motions reflect its diffusion within the bulk membrane followed by confinement within a domain that itself diffuses slowly and suggests that this confinement is due to interactions with the confining molecules. Alternatively, Ritchie et al. (124) suggest that these interactions may be with proteins forming a continuous barrier (fences) or discontinuous protein barrier (pickets). Fences or pickets can confine and limit receptor diffusion within small membrane regions while still permitting intermittent escape from a compartment zone followed by faster diffusion in the bulk membrane. Our previous studies of LH receptor lateral diffusion using fluorescence photobleaching recovery methods suggest that actin microfilaments may provide fences or organizing structures for pickets that restrict the lateral motions of the receptor (125). Nonetheless, one caveat in interpreting these results

is that the compartments occupied by hCG-occupied LH receptors should not be equated *a priori* with structures identified in biochemical studies such as plasma membrane rafts. The relationship of biochemically-identified rafts to membrane compartments visualized via single-particle tracking remains a topic of active debate.

Finally, disruption of the membrane rafts reduced, but did not completely eliminate, LH signaling. This result is reasonable if hormone-mediated signaling is most efficient within rafts where higher concentrations of downstream signaling molecules exist. Nonetheless, some signaling proteins remain available within the bulk membrane, albeit at reduced concentrations, where they are capable of relaying a productive signal. The questions that remain are what role receptor aggregation plays in signaling and raft localization, whether small membrane compartments accessed by hCG-occupied receptors are the same structures isolated in low density sucrose fractions, and whether rafts are essential for LH receptor function. These questions seem likely to be resolved only if it can be demonstrated that forcing an LH receptor, either with or without ligand, into the raft environment, can produce a downstream signal and if some, or all, of the components involved in LH-receptor mediated signaling can be localized with LH receptors in the same membrane compartments. Alternatively, raft localization may be a convenient, but not essential method, for concentrating membrane proteins involved in signal transduction.

Table 1: Tracking of individual anti-FLAG-gold particles bound to FLAG-LHR-wt on CHO cells.

Cell Line	Pretreatment	Hormone	Number of particles analyzed	Number of domains/ 2 min trajectory	$D_{0\text{-}1}$ [a] ($10^{-11}cm^2sec^{-1}$)	$D = L_r^2/4t$ [b] ($10^{-11}cm^2sec^{-1}$)	Time[d] (sec)	Domain Diameter (L_r)[c]
wt	none	none	20	6 ± 2	6.8 ± 3.8	1.2 ± 0.8	16 ± 13	230 ± 79
wt	none	hCG	20	5 ± 2	2.9 ± 1.1	0.1 ± 1.8	20 ± 11	86 ± 36
wt	MβCD	hCG	10	5 ± 1	4.8 ± 2.8	0.3 ± 0.8	19 ± 5	150 ± 12
wt	none	degly-hCG	10	2 ± 1	3.1 ± 1.9	3.4 ± 3.9	17 ± 14	256 ± 103
K583R	none	none	10	2 ± 1	3.3 ± 1.3	2.3 ± 2.2	27 ± 11	200 ± 92
K583R	none	hCG	10	2 ± 1	2.5 ± 4.0	1.8 ± 2.0	29 ± 11	164 ± 94

[a] $D_{0\text{-}1}$: Diffusion coefficient of the first 2 points.

[b] D presents the diffusion coefficient within a domain.

[c] The average diameter of an individual domain.

[d] Average time for residence within a domain

CHAPTER 4[3]

Compartmentalization of the Type I Fcε Receptor and MAFA on Mast Cell Membranes

ABSTRACT

The MAst cell Function-associated Antigen (MAFA) is a membrane glycoprotein on rat mast cells (RBL-2H3) expressed at a ratio of ~1:30 with respect to the Type I Fcε receptor (FcεRI). Despite this stoichiometry, clustering MAFA by its specific mAb G63 substantially inhibits secretion of both granular and *de novo* synthesized mediators induced upon FcεRI aggregation. Since the FcεRIs apparently signal from within raft micro-environments, we investigated possible co-localization of MAFA within these membrane compartments containing aggregated FcεRI. We used cholera toxin B subunit (CTB) to cluster the raft component ganglioside GM1 and studied the effects of this perturbation on rotation of FcεRI and MAFA by time-resolved phosphorescence anisotropy of erythrosin-conjugated probes. CTB treatment would be expected to substantially inhibit rotation of raft-associated molecules. Experimentally, CTB has no effect on rotational parameters such as the long-

---

3

This chapter has been adapted from B. George Barisas, Steven M. Smith, Jingjing Liu, Jinming Song, Guy M. Hagen, Israel Pecht and Deborah A. Roess (2006) Compartmentalization of the Type I Fcε Receptor and MAFA on Mast Cell Membranes Self-association and raft localization of functional luteinizing hormone receptors, *Biophysical Chemistry,* accepted for publication.

time anisotropy (r_∞) of unperturbed FcεRI or MAFA. However, on cells where FcεRI-IgE has previously been clustered by antigen (DNP_{14}-BSA), CTB treatment increases the FcεRI-IgE's r_∞ by 0.010 and MAFA's by 0.014. Similarly, CTB treatment of cells where MAFA had been clustered by mAb G63 increases MAFA's r_∞ by 0.010 but leaves FcεRI's unaffected. Evaluation of raft localization of FcεRI and MAFA using sucrose gradient ultracentrifugation of Triton X-100 treated membrane fragments demonstrates that a significant fraction of MAFA molecules sediments with rafts when FcεRI is clustered by antigen *or* when MAFA itself is clustered by mAb G63. The large excess of FcεRI over MAFA explains why clustering MAFA does not substantively affect FcεRI dynamics. Moreover, in single particle tracking studies of individual FcεRI-IgE or MAFA molecules, these proteins, upon clustering by antigen, move into small membrane compartments of reduced, but similar, dimensions. This provides additional indication of constitutive interactions between FcεRI and MAFA. Taken together, these results of distinct methodologies suggest that MAFA functions within raft microdomains of the RBL-2H3 cell membrane and thus in close proximity to the FcεRI which themselves signal from within the raft environment.

INTRODUCTION

The Type I Fcε receptors expressed on mast cells and basophils (FcεRI) are specific for the respective Fcε domains of IgE molecules and bind them with a stoichiometry of 1:1. Although binding by itself does not the initiate secretory response of these cells, clustering of the FcεRI via the bound IgEs which serve as antigen-specific, divalent adaptors provides the signal leading to the above cellular response (40). This response involves secretion of both granule-stored mediators such as histamine as well as the *de novo* synthesized ones (44) utilizing a signaling network that includes recruitment and activation of specific protein tyrosine kinases (PTK)(48), a transient increase in tyrosine phosphorylation of several cellular proteins (49, 50)and free intracellular calcium ion concentrations (126) and activation of PLCγ and phosphatidyl inositide hydrolysis (127).

Several membrane proteins, including a membrane glycoprotein termed the MAst cell Function-associated Antigen (MAFA), have been found to suppress the FcεRI-mediated secretory response(128-132) upon being clustered by the specific mAb G63. Although there is only approximately one MAFA expressed for every thirty FcεRI, clustering MAFA was shown to inhibit by up to 80% the secretory response of the rat mucosal-type mast cells of the RBL-2H3 line to subsequent FcεRI clustering (133). MAFA apparently delivers negative signals overriding those of the aggregated FcεRI upstream of PLCγ activation by suppressing both phosphatidylinositide phosphate hydrolysis and transient intracellular calcium elevation (133, 134) and these inhibitory effects are not due to MAFA interference with IgE-FcεRI interactions (133). Pecht and coworkers have shown that MAFA clustering induces

phosphorylation of the tyrosine residue of its immuno-receptor tyrosine-based inhibitory motif (ITIM) by the PTK *lyn* (135) . This induces recruitment to this ITIM of both SHIP, presumably causing reducion of PIP_3 levels (135), and SHP2, lowering *syk* activity (136).

Previous studies suggest functionally-significant interactions between FcεRI and MAFA within the cell membrane. Fluorescence resonance energy transfer measurements demonstrate proximity of FcεRI to MAFA binding mAb G63 (137). Time-resolved phosphorescence anisotropy measurements of rotational dynamics of FcεRI and MAFA (138) suggest that these molecules are constitutively associated with one another, at least to some extent, irrespective of MAFA's aggregation state. Thus it is important to determine whether these interactions occur at arbitrary sites in the plasma membrane or in well-defined membrane compartments. Membrane microdomains include so-called rafts which, because of their high cholesterol and sphingolipid content, float in sucrose gradients. Rafts are enriched, not only with sphingolipids and cholesterol (3), but also with glycosylphosphatidyl-inositol (GPI)-anchored proteins (93) and, in some cells, comprise a substantial fraction of the plasma membrane (18, 95). These microdomains can contain membrane proteins necessary for cell signaling (97) and have been reported to diffuse laterally as intact entities within the plasma membrane (94). Baird's group has shown that unperturbed, non-aggregated FcεRI are dispersed within the plasma membrane but, upon aggregation, are translocated into lipid rafts (139). To independently examine the effects of FcεRI clustering on the compartmentalization of MAFA or FcεRI, we have now combined several methods, time-resolved phosphorescence anisotropy measurements of protein rotation, density gradient ultracentrifugation and single particle tracking of individual protein molecules on viable cells

in order to evaluate the characteristics of membrane compartments accessed by MAFA and FcεRI.

MATERIALS AND METHODS

Cells and culture.

Rat mucosal-type mast cells of the RBL-2H3 line were kindly provided by Dr. Reuben Siraganian of the National Institutes of Health. Cells were grown and characterized as described (138) in Minimum Essential Medium Eagle with Earle's salts (VWR), containing HEPES buffer and non-essential amino acids (Sigma-Aldrich, St. Louis, MO) and supplemented with 10% fetal bovine serum (Gemini Bio Products, Woodland, CA). Cells were grown to approximately 90% confluence in BD Falcon non-treated, plug-seal tissue culture flasks (VWR), which they prefer, and then seeded into Petri dishes for high-throughput cell culture. For raft experiments, 20 dishes were usually grown to provide the necessary 25 million cells per sample. Cells were harvested from culture using a 5mM EDTA in PBS for 10 minutes at 4°C and then washed down using Hank's Balanced Salt Solution.

Antibodies, proteins and conjugates.

Monoclonal antibody G63 (IgG_1) was purified from hybridoma culture supernatants by chromatography (138). Monoclonal 2-4-dinitrophenyl (DNP)-specific A2 mouse IgE was purified from ascitic fluid by binding to DNP-Sepharose and elution with DNP-glycine (133). FcεRI alpha chain-specific antibody was obtained from Upstate Cell Signaling

Solutions, Lake Placid, NY. DNP_{14}-BSA, derivatized with an average of 14 DNP-groups per molecule, was prepared as described earlier (140). Antibodies were derivatized with erythrosin isothiocyanate (Er, Molecular Probes, Eugene, OR) using a modification (138) of methods described by Johnson and Holborow (141). Prior to use, all dye-derivatized proteins were centrifuged at 130,000x g for 10 min in a Beckman Airfuge (Beckman Instruments, Palo Alto, CA) to remove any protein aggregates formed during storage.

Time-resolved phosphorescence anisotropy measurements.

Time-resolved phosphorescence anisotropy (TPA) experiments were performed using methods previously described (142, 143) as adapted for MAFA (138). Cells were labeled either with erythrosin isothiocyanate (Er)-conjugated A2-IgE to monitor FcεRI or with Er-G63 Fab to monitor MAFA. Typical conditions were 150 nM and 30 nM, for FcεRI and MAFA respectively, for 1 hr at 4°C. Phosphorescence from deoxygenated cell samples (144) was excited by 532 nm pulses from a Nd:YAG laser. Phosphorescence emitted polarized parallel $I_{\parallel}(t)$ and perpendicular $I_{\perp}(t)$ to the exciting light were analyzed to yield a phosphorescence intensity function $s(t) = I_{\parallel}(t)+2I_{\perp}(t)$ and a phosphorescence anisotropy function $r(t)=[I_{\parallel}(t)-I_{\perp}(t)]/s(t)$. Anisotropy data were analyzed according to a single average exponential decay model $r(t)=r_{\infty} + (r_0-r_{\infty})\exp(-t/\varphi)$ which yielded the initial anisotropy value r_0, the limiting anisotropy value r_{∞} and the rotational correlation time φ (138).

Density-gradient fractionation of RBl- 2H3 cell membrane extracts.

To isolate membrane rafts from RBL-2H3 cells, 5 x 10^7 cells were washed two times with Hank's Balanced Salt Solution, pH 7.2 (BSS) and then lysed for 5-10 minutes on ice in 1ml of a buffer containing 25mM MES, 150mM NaCl, 2mM EDTA, 0.25% Triton-X100, and protease inhibitors including aprotinin, leupeptin, EDTA, and PMSF (Roche). 1 mL of the cell lysate solution containing plasma membrane fragments was then combined with 1mL of 80% sucrose to produce a 40% sucrose solution. A discontinuous sucrose gradient from 10-80% was created with the sample in 40% sucrose layered within this gradient. The gradient was loaded into a Beckman SW-41 swinging bucket rotor and spun at 175,000x g for 20 hours at 4°C . After the spin, eighteen 650 μL fractions were carefully collected from the top of the gradient downward. A 50 μL aliquot from each fraction was diluted 1:1 with 95% SDS and 5% β-mercaptoethanol. After separation of proteins from each fraction using SDS-PAGE and transfer of proteins to nitrocellulose, proteins of interest, MAFA and the FcεRI receptor were identified using 4-10 μg of the MAFA-specific antibody G63 or anti-FcεRI alpha chain antibody (Upstate Cell Signaling Solutions, Lake Placid, NY), respectively. Blots were incubated 5 min with "Super Signal West Pico" chemiluminescence detection substrate (3mL peroxide solution plus 3mL luminol enhancer solution (Pierce-Endogen, Rockford, IL) and recorded by 1-5 min exposure on Amersham Enhanced ECL film (Amersham Pharmacia Biotech, England). The amount of MAFA or receptor in each fraction was measured using a Bio-Rad GS-800 calibrated densitometer. The sucrose concentration in each fraction was determined using a Bausch and Lomb refractometer. For

all experiments, cells were pre-incubated with 100 ng/mL DNP-specific A2-IgE for 1 hour at 37°C prior to further treatment. FcεRI-IgE clustering was achieved in cells suspended in BSS by incubation with 100 nM of the antigen, DNP_{14}-BSA for 45 min at room temperature (52). Aggregation of MAFA was accomplished by treating cells MAFA-specific mAb G63 in BSS for 1 hr at 37°C.

Single-particle tracking of FLAG-LHR-wt receptors on individual cells.

Lateral dynamics and the size of domains accessed by individual FcεRI or MAFA were evaluated using single-particle tracking (SPT) methods as described by Kusumi and coworkers (59). 40 nm gold particles (Ted Pella, Inc., Redding, CA) were conjugated with IgE or mAb G63 or its Fab fragments, essentially as described by Daumas *et al.* (103) who estimated an average of two antibody molecules bound per nanoparticle. RBL-2H3 cells grown on a coverslip were then incubated with 100 μL of antibody-conjugated nanogold at a concentration of $9x10^{10}$ particles per mL for 1 hr at 4°C. This labeling typically produced 1-4 gold particles per cell. Binding of these mAbs was specific for either FcεRI or MAFA as, when cells were preincubated with a 10-fold excess of antibody, no particles were detected on the cells.

Individual nanoparticles were imaged by differential interference contrast using a 63x 1.4 NA oil immersion objective and a 1.4 NA oil condenser on a Zeiss Axiovert 135 microscope with a 2.5x Optovar and 2x C-mount adapter. Images were acquired using a Dage IFG-300 camera and were recorded for 2 min (3600 frames) at approximately 30

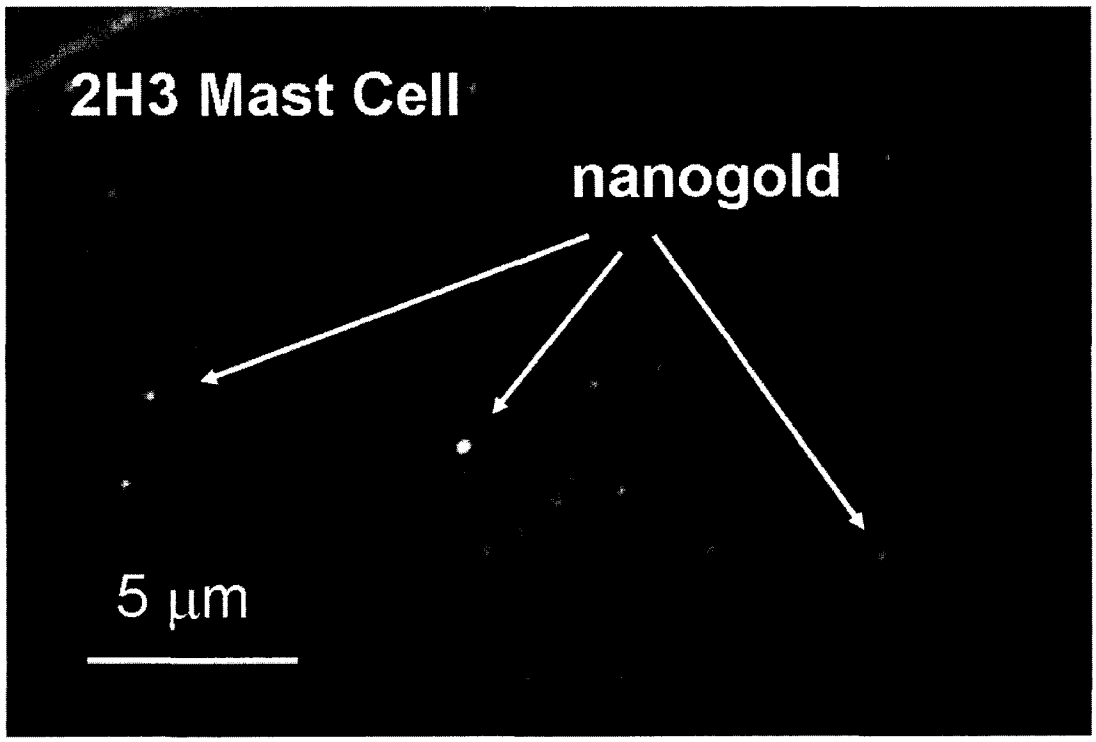

Figure 15: Photograph of 2H3 cell showing IgE-nanogold particles bound to individual Type I Fcε receptors

nm/pixel under the control of Metamorph software (Molecular Devices Corporation, Sunnyvale, CA). The trajectories for individual gold particles were segmented into compartments by calculation of statistical variance in particle position over times using a procedure similar to that developed by other investigators (102-104). The normalized variance s_i^2 of a particle's position (x_i, y_i) at a particular frame time i within a window of duration n frames was calculated as

$$s_i^2 = \frac{n\sum_{j=i-n/2}^{i+n/2-1} x_j^2 - \left(\sum_{j=i-n/2}^{i+n/2-1} x_j\right)^2}{n^2(n-1)} + \frac{n\sum_{j=i-n/2}^{i+n/2-1} y_j^2 - \left(\sum_{j=i-n/2}^{i+n/2-1} y_j\right)^2}{n^2(n-1)} \quad (1)$$

Translating windows along the particle trajectory produced plots where peaks indicate inter- compartment jumps and multiple plots for a range of window durations can be presented as a 3-dimensional graph such as shown in Figure 2. Such a graph allows individual inter-compartment jump times to be identified using whatever window length provides maximum information. The times of jumps thus identified were used to segment particle trajectories into discrete domains, such as shown in Figure 3. Segmented trajectories were then analyzed to yield the domain sizes and residence times for each particle. Residence times were calculated as the time between jumps, while the compartment diagonal was estimated as $[12(s_x^2+s_y^2)]^{1/2}$ where s_x^2 and s_y^2 are the x- and y-variances of particle position within each domain. Effective macroscopic diffusion constants were calculated as

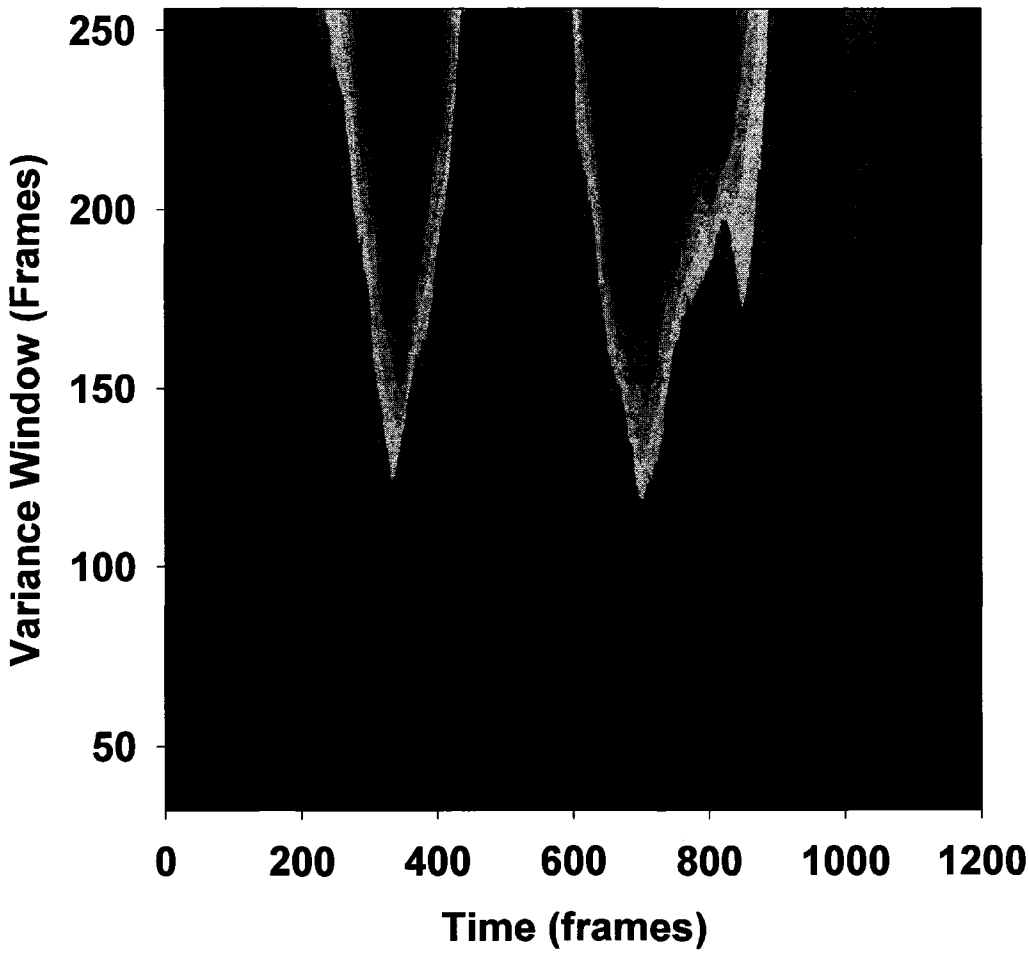

Figure 16: 3D plot of normalized variance of IgE-binding gold nanoparticle position on a 2H3 cell within time windows of durations ranging from 256 frames (top) to 32 frames (bottom). Windows are translated along particle trajectory. Times of inter-domain jumps are indicated by peaks.

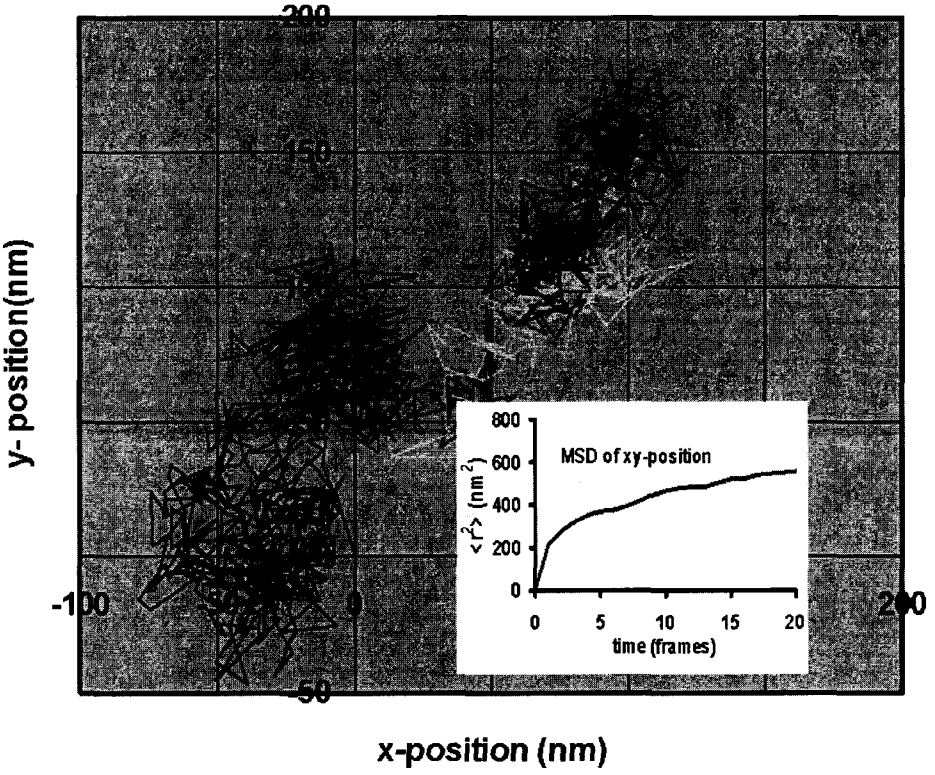

Figure 17: Segmentation of trajectory of a IgE-binding gold nanoparticle on a 2H3 cell into domain regions by the method shown in Figure 1. Analysis of the size of a domain and the particle residence time provides an estimate of the macroscopic diffusion coefficient expected for the receptors to which the particle attaches.

the square of the compartment diagonal L_t divided by four times the residence time τ in the compartment as previously described (104). Typically, 3-5 inter-compartment jumps were examined for each nanogold particle tracked.

RESULTS AND DISCUSSION

To explore possible MAFA-FcεRI interactions and their possible relation to MAFA's inhibition of secretion, we have previously studied by time-resolved phosphorescence anisotropy the rotational behavior of both MAFA and FcεRI in both unperturbed states and as ligated by various reagents involved in FcεRI-induced secretion and MAFA-mediated inhibition thereof (138, 145). From 4°C to 37°C the rotational correlation times of FcεRI-bound, erythrosin-conjugated IgE resemble those observed for MAFA-bound erythrosin-conjugated G63 Fab, 82±17 μs and 79±31 μs at 4°C, respectively. Clustering the FcεRI-IgE complex by antigen or by anti-IgE increases the phosphorescence anisotropy of G63 Fab and slows its rotational relaxation. Antigen clustering of the FcεRI-IgE complex has also been found to slow the lateral diffusion of cell-bound G63 Fab (138).

It has previously been demonstrated that clustering FcεRI causes the receptor to enter membrane raft microdomains (146). The ganglioside GM1 characterizes these domains and its clustering increases the ordering of raft lipids. Thus we induced extensive GM1 aggregation by treating cells with a CTB-biotin conjugate followed by addition of streptavidin and examined the impact of this aggregation on the rotation of FcεRI and MAFA. Key results of these experiments are summarized in Table I while a sample experimental trace is shown in Figure 4. In this figure, the lower trace depicts anisotropy decay, and hence rotation, of FcεRI binding phosphorescent Er-IgE and clustered by DNP_{14}-BSA. The upper trace shows anisotropy decay for a similar sample but additionally treated, before measurement, with CTB-biotin and streptavidin to aggregate GM1. This GM1

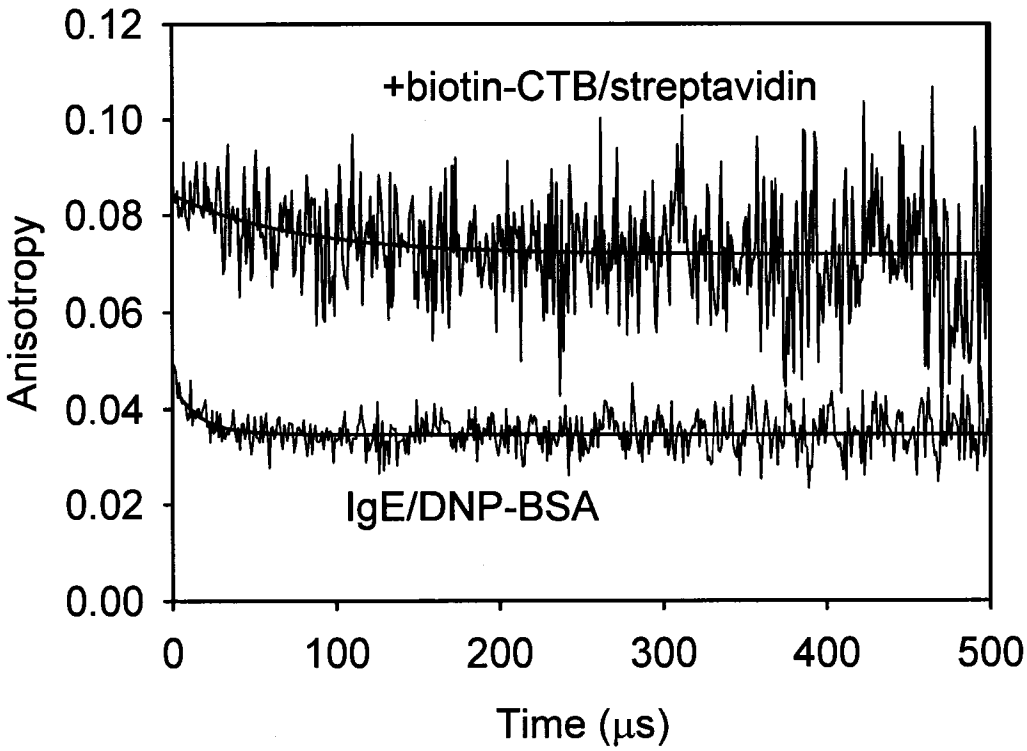

Figure 18: Effect of CTB treatment on rotation of A2 IgE-binding FcεRI aggregated by DNP-BSA. Time-resolved phosphorescence anisotropy measurements of protein rotation were performed at 4°C as described in the text. The increased limiting anisotropy induced by CTB suggests that the aggregated FcεRI are associated with raft microdomains.

aggregation produces a substantial increase in limiting anisotropy r_∞ of the aggregated IgE-FcεRI, indicating that a considerable fraction of receptors have been rotationally immobilized. This is to be expected since, as described earlier, DNP-BSA aggregated receptors are known to translocate into lipid rafts where their mobility would be restricted by ordering of the raft lipid GM1. Table I summarizes the results of the entire series of such experiments. In each line, the entry in first column indicates which membrane molecule was aggregated prior to measurements included on that line of the table. The next three columns indicate, for FcεRI rotation on cells thus pre-treated, the limiting anisotropies observed on otherwise untreated cells, on cells treated with biotin-CTB and streptavidin just prior to rotation measurements and the anisotropy difference resulting from CTB treatment. The last three columns indicate the same data for MAFA rotation. CTB treatment significantly increases r_∞ only for the FcεRI-IgE that have been pre-clustered by antigen as shown in column 4. However, pre-clustering *either* FcεRI by antigen treatment *or* MAFA by G63 Fab and second antibody increases MAFA's r_∞ as shown in column 7. This would be explained if MAFA is pre-associated with the receptor and hence enters rafts when either species is aggregated. By this argument, aggregating MAFA would also translocate some receptors into rafts. However, since there is only one MAFA for every 30 receptors, the fractional increase in the receptors' measured r_∞ would be undetectable. Thus, these rotational diffusion studies are consistent with the notion that both MAFA and FcεRI preferentially translocate into raft domains, upon being clustered.

To explore raft localization of MAFA and FcεRI in more detail, we have isolated plasma membrane rafts from RBL-2H3 cells using reported standard methods and examined

conditions under which both MAFA and FcεRI appear in these microdomains. Figure 5 presents western blots of FcεRI and MAFA in different sucrose fractions after density gradient fractionation of detergent extracts from variously-treated cells. As can be seen in the figure, there is a substantially larger amount of FcεRI in low buoyant density fractions, *i.e.* raft fractions, after clustering by antigen. Table II shows quantitative densitometric analysis of a number of such experiments. As was suggested by results of the rotation experiments described above, both DNP_{14}-BSA clustering of FcεRI-IgE and G63 clustering of MAFA cause substantially increased amounts of MAFA to appear in low-density plasma membrane fractions. Similarly, the amount of FcεRI found in membrane rafts is significantly increased upon FcεRI clustering with DNP_{14}-BSA, as shown previously by Baird and coworkers (146). However, clustering MAFA with mAb G63 does not significantly increase the apparent amount FcεRI in raft fractions. This result is also consistent with constitutive MAFA interactions with the FcεRI receptor and with the known relative excess of FcεRI over MAFA. Thus, G63-clustered MAFA moves into rafts but, presumably each MAFA can bring only one FcεRI, or about 1/30 of the total available FcεRI, into these domains. One would not expect such a small change in the distribution FcεRI to be detectable in experiments such as these.

We then explored the lateral localization of individual MAFA and FcεRI molecules by means of single-particle tracking. IgE-nanogold, G63 Fab-nanogold and G63 mAb-nanogold probes were employed to examine the motions of FcεRI and MAFA, respectively. DNP_{14}-BSA treatment was used to cluster the receptors while intact mAb G63-nanogold

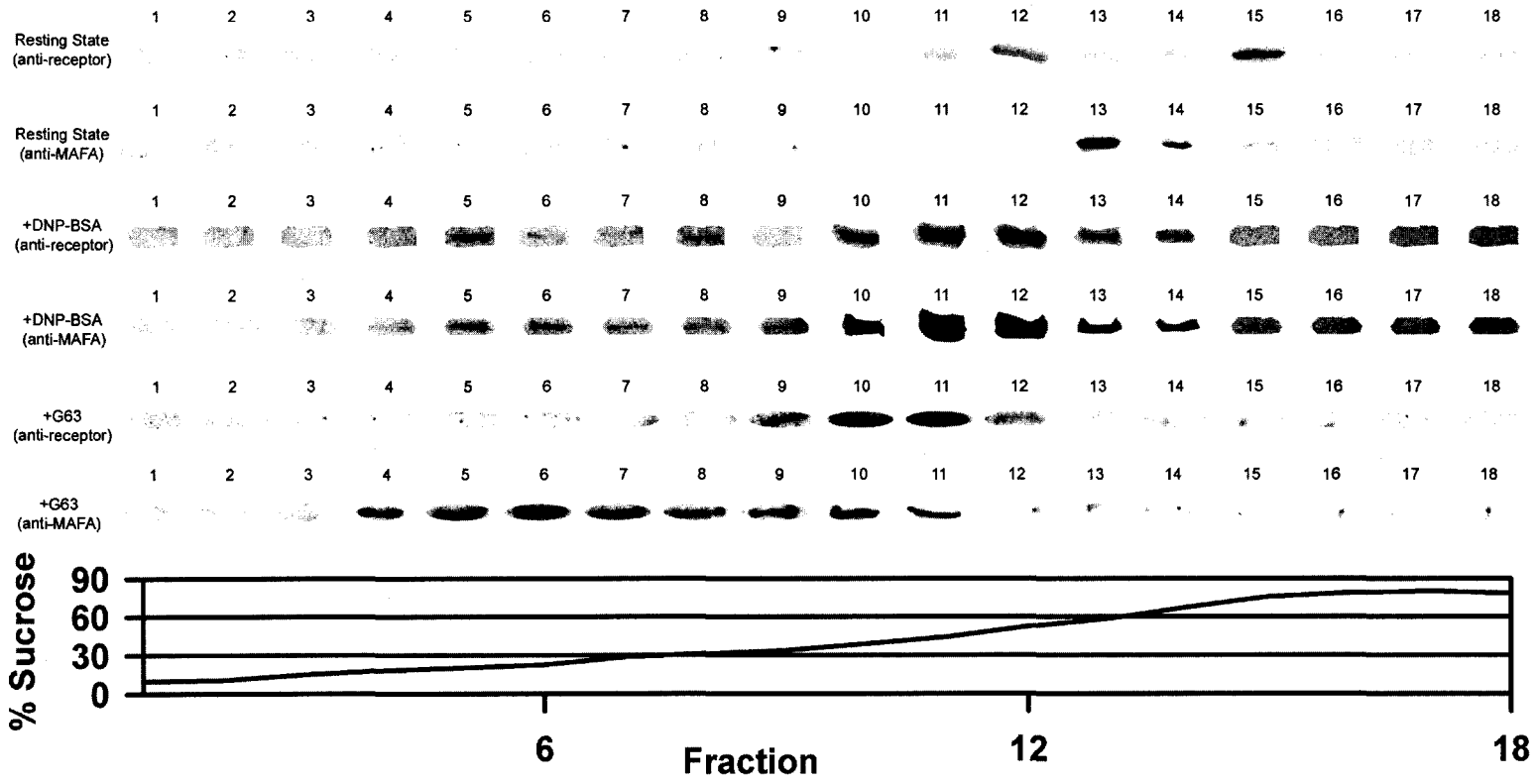

Figure 19: Detection of aggregated MAFA and FcεRI in low-density regions of sucrose gradients following ultracentrifugation of 2H3 cell membrane detergent extracts. Representative western blots obtained demonstrate that FcεRI (panels 1, 3 and 5) is located in high buoyancy membrane fractions only after crosslinking of receptor with DNP_{14}-BSA while MAFA (2, 4, and 6) moves into low-density membrane fractions after treatment of cells with either G63 antibody or crosslinking of FcεRI by DNP_{14}-BSA.

probes presumably indicated motions of clustered MAFA. Calculation of the variance of particle position over various-sized time windows (Figure 2) allowed segmentation of trajectory into individual compartments as shown in Figure 3. The segmented trajectories were then analyzed to yield the diffusion coefficient D_{01} for mobility within each compartment, the residence time τ of particles in compartments, the compartment size L_r and the diffusion coefficient D_{hop} for hop diffusion between compartments. A summary of these results is shown in Table III. On un-perturbed cells, the average compartment containing either FcεRI or MAFA was approximately 160nm in diameter. However, specific clustering of either MAFA by G63 or FcεRI by DNP_{14}-BSA reduced the compartment size accessed by these molecules to 90 nm and 53 nm, respectively, though the residence time of receptors within these compartments remains essentially constant at about 20 sec. The shift in the distribution of compartment sizes from large to small upon receptor clustering is more clearly depicted in Figures 6 and 7 which show histograms of compartment sizes exhibited by FcεRI and MAFA on variously-treated cells, respectively.

In a separate set of experiments, we examined the effects of CTB pre-treatment on single-particle dynamics of the FcεRI and MAFA under conditions analogous to those used for measuring FcεRI and MAFA rotation as discussed above. Cells were pre-treated with CTB (5 μg/ml for 50 min at 4°C), bound with IgE- or G63-nanogold (50 min at 4°C) and finally treated with antigen or buffer (40 min at 4°C). Results of these experiments are shown in Table IV. These results suggest that CTB pre-treatment hinders the antigen-induced movement of both FcεRI and MAFA into smaller membrane compartments since DNP_{14}-BSA treatment does not significantly reduce the compartment size accessed by either

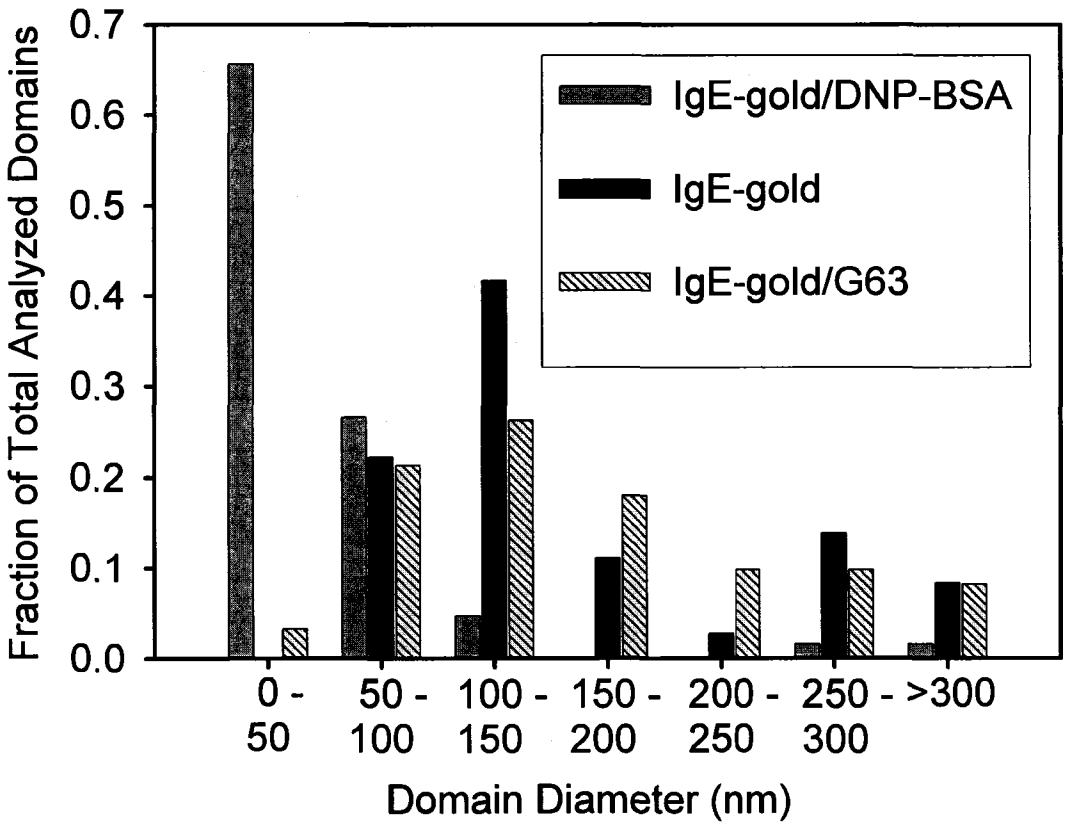

Figure 20: Distribution of compartment sizes from single particle tracking of FcεRI. Individual values for compartment size calculated from particle tracks of FcεRI before and after crosslinking of FcεRI with DNP_{14}-BSA or crosslinking of MAFA with G63 antibody. Only DNP_{14}-BSA crosslinking moved FcεRI into smaller membrane compartments with 88% of receptors appearing in compartments with diameters of less than 75nm.

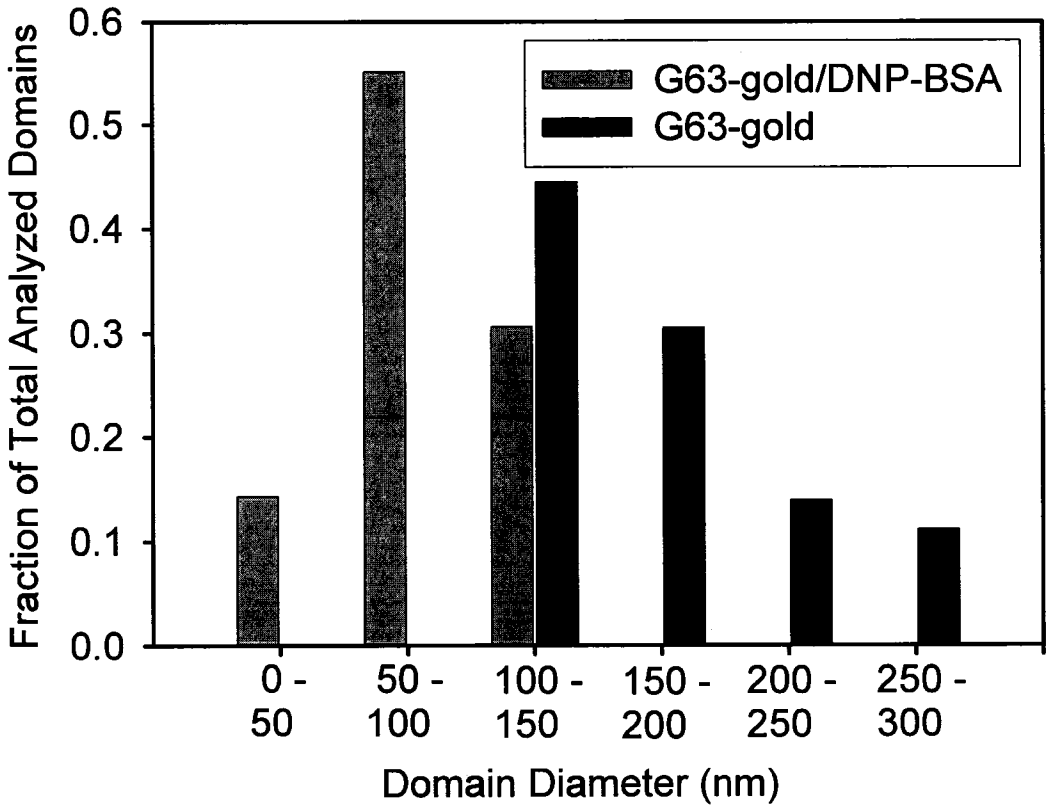

Figure 21: Distribution of values for compartment size from single particle tracking of MAFA. Individual values for compartment sizes were calculated from particle tracks of MAFA before and after crosslinking of FcεRI with DNP_{14}-BSA.

receptor. This would be expected if CTB binding to GM1 substantially increases raft lipid ordering which might, in turn, slow or restrict subsequent entry of aggregated FcεRI or MAFA into rafts. These molecules would then retain greater freedom from corralling by sub-membrane structures and so continue to access that same large compartments as before aggregation.

Results of the preceding SPT experiments raise the question of how the large and relatively stable compartments accessed by the receptors in these experiments may relate to possible localization of receptors in raft microdomains. While various estimates of raft size have earlier been put forward, recent high-speed single-particle tracking studies by Kusumi (102) suggest that 30-230 nm transient confinement zones observed for membrane lipids, with residence times of 1-17 ms, may be equated with rafts. However, the large compartments observed on much slower timescales, such as in the present study, must reflect different cell membrane structures. We have noted previously that, for various membrane species on the same cell, the residence time of these proteins in compartments tends to be relatively constant (54, 147). This would be the case if different dynamic structures, perhaps a cytoskeletal network, beneath the plasma membrane restricted or "corralled" membrane receptors for much of the time but fluctuated from time to time in their stability or in their association with the plasma membrane and so allowed membrane-resident molecules to escape. Raft microdomains would be expected to involve substantial concentration of signaling-related molecules such as kinases at the cytoplasmic face of the membrane. Thus, raft-associated species, such as FcεRI and MAFA after antigen treatment, might well prove more susceptible to compartmentalization by cytoskeletal structures than corresponding

molecules in the bulk membrane and thus exhibit smaller average compartment sizes.

A key question concerning MAFA action is how is the relatively small number of MAFA molecules capable of such effective inhibition of cellular responses to FcεRI signaling. Several lines of work have indicated that MAFA is, to some extent, constitutively pre-associated with FceRI on unperturbed 2H3 cells (137, 145, 148). Moreover, co-clustering FceRI and MAFA using bispecific reagents has been shown to provide more effective inhibition than MAFA clustering alone (149, 150). *Lyn* phosphorylation of MAFA's ITIM provides the site for recruitment and activation of the inhibitory phosphatase SHIP which depletes PLCγ reaction substrate (135) and for the protein tyrosine phosphatase SHP2 (136). Since FcεRI signaling derives from receptor ITAM-specific phosphorylation in rafts by *lyn*, raft-associated receptors should provide sites of increased *lyn* concentration. Both because *lyn* activity is highest within lipid rafts and because of the presumed small dimensions of rafts, any translocation of MAFA into rafts could cause an enhanced inhibitory effect. Moreover, MAFA co-aggregated with FcεRI might encounter an even higher local concentration of *lyn* than separately clustered MAFA. This would amplify the inhibitory process by having *lyn* produce additional phosphorylation of the MAFA ITIM and the increase subsequent recruitment and activation of SHIP. Further, recent studies have shown that FcεRI phosphorylation reflects a dynamic balance between intrinsic *lyn* activity and FcεRI dephosphorylation by phosphatases such as SHP-1 (151). Thus MAFA co-aggregated with the receptor might additionally contribute to reduced steady-state receptor phosphorylation.

Table 2. Effects of cholera toxin treatment on the limiting rotational anisotropy of FcεRI and MAFA, with and without pre-crosslinking by DNP-BSA and anti-G63 Fab[a]

Protein Aggregated Initially[b]	Membrane Species for which Rotational Limiting Anisotropy (r_∞) Measured Subsequently					
	Er-IgE-FcεRI			Er-G63 Fab-MAFA		
	no CTB (control)	CTB-treated	r_∞ Change caused by CTB	no CTB (control)	CTB-treated	r_∞ Change caused by CTB
none	0.046	0.046	0	0.048	0.047	0
FcεRI	0.062	0.072	+0.010[c]	0.047	0.061	+0.014[c]
MAFA	0.059	0.057	0	0.051	0.061	+0.010[c]

[a] The labeling sequence was 1) 150 nm unlabeled-IgE or Er-IgE at 4°C for 1 hr; 2) for measuring MAFA rotation and/or MAFA crosslinking, 30 nm Er-G63Fab or 30 nm unlabeled G63Fab, respectively, at 4°C for 1 hr; 3) FcεRI or MAFA crosslinking by treatment with 14 μg/ml DNP_{14}-BSA at 4°C for 1 hr or 4 μg/ml goat anti-mouse Fab at 37°C for ½ hr, respectively; and,finally, 4) 5 μg/ml biotin-cholera toxin subunit B at 4°C for 1 hr followed by 4 μg/ml streptavidin at 37°C for 5 min or comparable control incubation in buffer.

[b] All FcεRI were initially saturated with DNP-specific A2-IgE. When required, FcεRI were aggregated by treatment with DNP_{14}-BSA and MAFA was aggregated by treatment with monovalent G63 Fab fragments followed by goat anti-mouse Fab, respectively, as described above.

[c] Shaded values indicate circumstances where CTB treatment produced a significant increase in the limiting rotational anisotropy of the membrane species probed.

Table 3: Fractions of MAFA and FcεRI in present in low- and high-density membrane fractions extracted from variously-treated cells[1]

Treatment Number	Protein Blotted	% Protein in 10-34% sucrose[2]	% Protein in 39-80% sucrose	replicate expts.
none	FcεRI	16 ± 4	84 ± 4	2
none	MAFA	4 ± 1	96 ± 1	2
mAb G63	FcεRI	18 ± 5	82 ± 5	4
mAb G63	MAFA	42 ± 8	58 ± 8	3
DNP_{14}-BSA	FcεRI	40 ± 2	60 ± 2	3
DNP_{14}-BSA	MAFA	40 ± 7	60 ± 7	3

[1] Western blots from variously-treated cells, such as those shown in Figure 4, were subjected to quantitative densitometry to determine the fractions of MAFA and FcεRI present in low-density (10-34% sucrose) and high-density (39-80% sucrose) membrane fractions.

[2] Proteins banding within range of sucrose densities are typically described as lipid raft-associated. The first three entries are nominally unperturbed molecular species while the last three entries are dimerized (mAb G63 treatment prior to MAFA blot) or highly aggregated (DNP_{14}-BSA treatment prior to FcεRI or MAFA blot). One-tailed t-tests indicate that FcεRI aggregation significantly ($p<0.01$) increases the fraction of both FcεRI (lines 5 *vs.* 1) and MAFA (lines 5 *vs.* 2) present in low density (raft) fractions while MAFA aggregation significantly increases only MAFA in rafts (lines 4 *vs.* 2).

Table 4: Single-particle tracking of individual FcεRI or MAFA before and after crosslinking with DNP_{14}-BSA or G63 antibody

Pretreatment	Nangold Conjugate	Number of particles analyzed	$D_{0\text{-}1}$ [a, b] ($10^{-11}cm^2sec^{-1}$)	D_{hop} [a, c] ($10^{-11}cm^2sec^{-1}$)	Residence Time τ [a, d] (sec)	Compartment Diameter L_r [a, e] (nm)
none	IgE	25	1.1 ± 0.7	0.30 ± 0.12	22 ± 16	163 ± 87
DNP_{14}-BSA	IgE	27	0.5 ±0.4	0.03 ± 0.05	24 ± 14	53 ± 53
G63	IgE	26	1.0 ± 0.4	0.26 ± 0.11	24 ± 15	160 ± 83
none	G63 Fab	13	5.8 ± 1.4	0.42 ± 0.12	16 ± 9	164 ± 67
none	G63 mAb	24	1.0 ± 0.4	0.23 ± 0.11	24 ± 16	149 ± 83
DNP_{14}-BSA	G63 mAb	26	0.9 ± 0.1	0.09 ± 0.02	23 ± 12	90 ± 31

[a] All uncertainties are presented as standard deviations (SD) of data sets, *not* as standard errors of means (SEM).

[b] Diffusion coefficient within compartment calculated from first two points of MSD vs. time plot [34].

[c] Diffusion coefficient for hop diffusion between compartments as calculated from compartment size L and particle residence time τ as $L^2/4\tau$ [36].

[d] Average particle residence time within a compartment.

[e] The average diameter of an individual compartment calculated as described by Daumas et al. [34] and Murase et al. [35].

Table 5: Combined Effects of CTB and DNP-BSA pretreatments on SPT measurements of FcεRI and MAFA dynamics

Pretreatment	Nangold Conjugate	Number of particles analyzed	$D_{0\text{-}1}$ [a, b] ($10^{-11}cm^2sec^{-1}$)	D_{hop} [a, c] ($10^{-11}cm^2sec^{-1}$)	Residence Time τ [a, d] (sec)	Compartment Diameter L_r [a, e] (nm)
CTB	IgE	10	3.0 ± 2.4	0.38 ± 0.17	29 ± 16	210 ± 104
CTB, DNP_{14}-BSA	IgE	10	2.1 ± 1.2	0.21 ± 0.06	33 ± 21	167 ± 69
CTB	G63	10	1.9 ± 0.8	0.20 ± 0.01	33 ± 17	162 ± 27
CTB, DNP_{14}-BSA	G63	10	2.6 ± 2.0	0.32 ± 0.20	34 ± 17	209 ± 115

[a] All uncertainties are presented as standard deviations (SD) of data sets, *not* as standard errors of means (SEM).

[b] Diffusion coefficient within compartment calculated from first two points of MSD vs. time plot [34].

[c] Diffusion coefficient for hop diffusion between compartments as calculated from compartment size L and particle residence time τ as $L^2/4\tau$ [36].

[d] Average particle residence time within a compartment.

[e] The average diameter of an individual compartment calculated as described by Daumas et al. [34] and Murase et al. [35].

CHAPTER 5

Discussion and Future Directions

Studies of membrane localization of the luteinizing hormone receptor and the high-affinity IgE receptor provide useful insights into two physiological relevant cellular signaling systems. Though these two membrane molecules are different in structure, function and mechanism by which they elicit a cellular response, these receptors require the cholesterol-enriched lipid raft environment during signaling events. The use of other methods, including single-particle tracking, supports the presence of small compartments within the membrane and the redistribution of membrane proteins into these small compartments following binding of ligand, as in the case of LHR, or extensive crosslinking, as is the case for the FcεRI and MAFA.

There are, however, a number of questions that have not been addressed in these studies are which are beyond the scope of this project.

1. As shown in Figure 7 in Chapter 2, it appears that LHR are present as self-associated receptor complexes within rafts following the binding of ligand. However, the order of events involved in aggregation of LHR and translocation to rafts is not known. It is possible that receptor-receptor interactions occur within the bulk membrane and that, after formation of receptors into dimers or oligomers, these complexes then translocate to rafts where they encounter other proteins involved in signaling and form large protein-containing

structures. There are strategies that may be effective in establishing the order of events leading to LHR clusters in rafts. One raft component, the ganglioside GM1, can be extensively crosslinked using cholera toxin. This crosslinking effectively excludes protein translocation into the raft structure. Thus biotin-cholera toxin and avidin crosslinking of GM1 together with further energy transfer studies might establish whether LHRs interact in the bulk plasma membrane or, alternatively, whether monomeric receptors move into lipid rafts where they self-associate. Crosslinking GM1 would also be useful in evaluating whether receptor signaling was impaired when receptors were excluded from rafts. These experiments would be tricky as cholera toxin activates cell signaling. However, there are now fluorescent cAMP reporters that make it possible to separate cAMP activation in cholera toxin-treated membrane microdomains from cAMP induced by LHR present in the bulk membrane.

2. LHRs undergo receptor desensitization after binding of ligand and, as shown by Roess et al. (69), do not respond to hormone challenge until self-associated receptors have dissociated and, based on lateral dynamics, moved back into the bulk membrane. This takes approximately five hours. These observations beg the question as to whether receptors remain in raft structures while desensitized. Perhaps one role of raft structures is to facilitate desensitization of LH receptors, possibly by encouraging interactions between receptor clusters and β-arrestin, an important mediator in receptor attenuation. Time-dependent evaluation of LHR localization in rafts following receptor desensitization would address this question as would probing for β-arrestin in membrane rafts.

3. We have not examined the effects of re-loading cholesterol using MβCD into membranes following cholesterol depletion. Presumably, the addition of cholesterol to membrane would cause re-formation of membrane compartments, something that could be shown in single-particle tracking experiments, and the reconstitution of effective signaling in response to ligand. These studies would support the notion that membrane compartments are necessary for effective LHR-mediated signaling.

4. We have demonstrated that rafts are present and functional in CHO cells. However, it would be valuable to repeat these studies using primary cultured granulosa cells or luteal cells. These experiments have been hindered by the lack of a reliable, commercially available antibody for the receptor. However, genetically engineered animals expressing epitope tagged LH receptors might make these experiments feasible.

5. An evaluation of fluorescence resonance energy transfer between LHR and membrane rafts components such as GM1 would further strengthen arguments that LHR are present in plasma membrane rafts during signaling. FRET evaluation between GM1 and LHR would be feasible. We would anticipate that there was no energy transfer between the LHR and GM1 prior to binding of ligand. Only upon addition of hormone would measurable levels of energy transfer be seen and this FRET would be eliminated by MβCD treatment.

6. For studies of FcεRI and MAFA activation, it would be very desirable to crosslink MAFA using a ligand other than G63. The physiological ligand for MAFA is not

known although there are recent indications that it may be a cytokine. Using a membrane permeable crosslinking agent or another mechanical crosslinker would be interesting.

REFERENCES

1. **Simons K, Ikonen E** 1997 Functional rafts in cell membranes. Nature 387:569-572
2. **Singer SJ, Nicolson GL** 1972 The fluid mosaic model of the structure of cell membranes. Cell membranes are viewed as two-dimensional solutions of oriented globular proteins and lipids. Science 175:720-731
3. **Brown DA, London E** 1998 Structure and origin of ordered lipid domains in biological membranes. Journal of Membrane Biology 164:103-114
4. **Poo M-M, Cone RA** 1974 Lateral diffusion of rhodopsin in the photoreceptor membrane. Nature 247:438-441
5. **Axelrod D, Koppel DE, Schlessinger J, Elson E, Webb WW** 1976 Mobility measurement by analysis of fluorescence photobleaching recovery kinetics. Biophysical Journal 16:1055-1069
6. **Jacobson K, Wu E, Poste G** 1976 Measurement of the translational mobility of con-canavalin A in glycerol-saline solutions and on the cell surface by fluorescence recovery after photobleaching. Biochimica et Biophysica Acta 433:215-222
7. **Leuther MD, Barisas BG, Peacock JS, Krakauer H** 1979 Photobleaching recovery studies of membrane events accompanying lectin stimulation of rabbit lymphocytes. Biochemical and Biophysical Research Communications 89:85-
8. **Wang Y-L, Lanni F, McNeil PL, Ware BR, Taylor DL** 1982 Mobility of cytoplasmic and membrane-associated actin in living cells. Proceedings of the National Academy of Science (USA) 79:4660-4664

9. **Goodwin JS, Kenworthy AK** 2005 Photobleaching approaches to investigate diffusional mobility and trafficking of Ras in living cells. Methods 37:154-164

10. **Zhang F, Lee GM, Jacobson K** 1993 Protein lateral mobility as a reflection of membrane microstructure. BioEssays 15:579-588

11. **Jacobson K, Sheets ED, Simson R** 1995 Revisiting the Fluid Mosaic Model of Membranes. Science 268:1441-1442

12. **Sheets ED, Holowka D, Baird B** 1999 Membrane organization in immunoglobulin E receptor signaling. Current Opinion in Chemical Biology 3:95-99

13. **Oh P, Schnitzer JE** 2001 Segregation of heterotrimeric G proteins in cell surface microdomains. Molecular Biology of the Cell 12:685-698

14. **Dietrich C, Volovyk Z, Levi M, Thompson N, Jacobson K** 2001 Partitioning of Thy-1, GM1, and cross-linked phospholipid analogs into lipid rafts reconstituted in supported model membrane monolayers. PNAS 98

15. **Lisanti MP, Sargiacomo M, Graeve L, Saltiel A, Rodriguez-Boulan E** 1988 Polarized apical distribution of glycosyl-phosphatidylinositol-anchored proteins in a renal epithelial cell line. Proc Natl Acad Sci U S A 85:9557-9561

16. **Cinek T, Horejsi V** 1992 The nature of large noncovalent complexes containing glycosyl-phosphatidylinositol-anchored membrane glycoproteins and protein tyrosine kinases. J Immunol 149:2262-2270

17. **Simons K, Toomre D** 2000 Lipid rafts and signal transduction. Nature Reviews, Molecular Cell Biology 1:31-39

18. **Maxfield FR** 2002 Plasma membrane microdomains. Curr Opin Cell Biol 14:483-

487

19. **Hansen GH** 2000 Cholesterol Depletion of Enterocytes. J Biol Chem 275:5136-5142

20. **Gether U** 2000 Uncovering molecular mechanisms involved in activation of G protein-coupled receptors. Endocrine Reviews 21:90-113

21. **Palczewski K, Kumasaka T, Hori T, et al.** 2000 Crystal structure of rhodopsin: a G protein-coupled receptor. Science 289:739-745

22. **Lefkowitz RJ** 1998 G protein-coupled receptors. Journal of Biological Chemistry 273:18677-18680

23. **McFarland K, Sprengel R, Phillips H, et al.** 1989 Lutropin-choriogonadotropin receptor: An unusual member of the G protein-coupled receptor family. Science 245:494-499

24. **Probst WC, Snyder LA, Schuster DI, Brosius J, Sealfon SC** 1992 Sequence alignment of the G-protein coupled receptor superfamily. DNA and Cell Biology 11:1-20

25. **Ascoli M, Segaloff D** 1989 On the structure of the luteinizing hormone/chorionic gonadotropin receptor. Endocrine Reviews 10:27-44

26. **Bousfield G, Liu W, Ward D** 1989 Effects of removal of carboxy-terminal extention from equine lutenizing hormone (LH) β-subunit on LH and follicle-stimulating hormone receptor-binding activities an LH steroidogenic activity in rat testicular Leydig cells. Endocrinology 124:379-387

27. **Conn PM, Huckel WR, Andrews WV, McArdle CA** 1987 The molecular mechanism of action of gonadotropin releasing hormone (GnRH) in the pituitary.

Recent Progress in Hormone Research 43:29-68

28. **Welt C, Sidis Y, Keutman H, Schneyer A** 2002 Activins, inhibins, follistatins: from endocrinology to signaling. A paradigm for the new millennium. European Journal of Biochemistry:724-752

29. **Cabrera-Vera T, Vanhauwe J, Thomas T, et al.** 2003 Insights into G protein structure, function, and regulation. Endocrine Reviews 24:765-81

30. **Gurevich VV, Chen CY, Kim CM, Benovic JL** 1994 Visual arrestin binding to rhodopsin. Intramolecular interaction between the basic N terminus and acidic C terminus of arrestin may regulate binding selectivity. J Biol Chem 269:8721-7

31. **Zhang J, Barak LS, Winkler KE, Caron MG, Ferguson SG** 1997 A central role for β-arrestins and clathrin-coated vesicle-mediated endocytosis in β_2-adrenergic receptor resensitization. Journal of Biological Chemistry 272:27005-27014

32. **Ferguson SSG, Downey III WE, Colopietro A, Barak LS, Menard L, Caron MG** 1996 Role of 225 β-arrestin in mediating agonist-promoted G protein-coupled receptor internalization. Science 271:363-365

33. **Shenker A** Disorders caused by mutations of the lutropin/choriogonadotropin receptor gene. In: Spiegel A (ed) Contemporary Endocrinology: G Proteins, Receptors and Disease. Humana Press, Totowa, NJ, pp 139-149

34. **Liu G, Duranteau L, Carel J-C, Monroe J, Doyle DA, Shenker A** 1999 Leydig-cell tumors caused by an activating mutation of the gene encoding the luteinizing hormone receptor. The New England Journal of Medicine 341:1731-1736

35. **Hébert TE, Bouvier M** 1998 Structural and functional aspects of G protein-coupled

receptor oligomerization. Biochemistry and Cell Biology 76, no. 1:1-11

36. **Horvat RD, Barisas BG, Roess DA** 2001 Luteinizing hormone receptors are self-associated in slowly diffusing complexes during receptor desensitization. Molecular Endocrinology 15:534-542

37. **Roess DA, Horvat RD, Clay C, Nelson S, Barisas BG** 1999 Binding of LH or hCG to an intrinsically fluorescent LH/hCG receptor leads to receptor aggregation and slow lateral diffusion. Annual Meeting of the Endocrine Society

38. **Patterson GH, Piston DW, Barisas BG** 2000 Förster distances between green fluorescent protein pairs. Analytical Biochemistry 284:438-440

39. **Lei Y, Hagen G, Smith S, Liu J, Barisas BG, Roess D** 2006 Constitutively-active human LH receptors are self-associated and localized in rafts. Molecular and Cellular Endocrinology:, in press

40. **DeLisi C** 1980 The biophysics of ligand-receptor interactions. Quarterly Reviews of Biophysics 13:201-230

41. **Ishizaka T, Chang TH, Taggart M, Ishizaka K** 1977 Histamine release from rat mast cells by antibodies against basophilic leukemia cell membrane. The Journal of Immunology 119:1589-1596

42. **Barsumian EL, Isersky C, Petrino MG, Siraganian RP** 1981 IgE-induced histamine release from rat basophilic leukemia cell lines: Isolation of releasing and nonreleasing clones. European Journal of Immunology 11:317-323

43. **Soto EO** 1990 Monoclonal Antibodies as Probes in the Study of Transmembrane Signaling in Mast Cells. Weizmann Institue of Science, Rehovot, Israel

44. **Schwartz L** 1994 Mast cells: function and contents. Current Opinions in Immunology 6:91-97

45. **Ortega E, Hazan B, Zor U, Pecht I** 1989 Mast cell stimulation by monoclonal antibodies specific for the Fcε receptor yields distinct responses of arachidonic acid and leukotriene C_4 secretion. European Journal of Immunology 19:2251-2256

46. **Bradding P, Feather I, Wilson S, et al.** 1993 Immunolocalization of cytokines in the nasal mucosa of normal and perennial rhinitic subjects. The Journal of Immunology 151:3853-3865

47. **Galli SJ, Gordon JR, Wershil BK** 1991 Cytokine production by mast and basophils. [review]. Current Opinions in Immunology 3:865-872

48. **Eiseman E, Bolen JB** 1992 Engagement of the high affinity IgE receptor activates SRC protein related tyrosine kinases. Nature 355:78-80

49. **Scharenberg AM, Lin S, Cuenod B, Yamamura H, Kinet J** 1995 Reconstitution of interactions between tyrosine kinases and the high affinity IgE receptor which are controlled by receptor clustering. The EMBO Journal 14:3385-3394

50. **Benhamou M, Gutkind JS, Robbins KC, Siraganian RP** 1990 Tyrosine phosphorylation coupled to IgE receptor-mediated signal transduction and histamine release. Proceedings of the National Academy of Science (USA) 87:5327-5330

51. **Ravetch JV, Kinet J-P** 1991 Fc Receptors. Annual Review of Immunology 9:457-492

52. **Sheets ED, Holowka D, Baird B** 1999 Critical role for cholesterol in Lyn-mediated tyrosine phosphorylation of FcεRI and their association with detergent-resistant

membranes. Journal of Cell Biology 145:877-87

53. **Oretega SF, Pecht I** 1988 A monoclonal antibody that inhibits secretion from rat basophilic leukemia cells and binds to a novel membrane component. The Journal of Immunology 141:4324-4332

54. **Kusumi A, Sako Y, Yamamoto M** 1993 Confined lateral diffusion of membrane receptors as studied by single particle tracking (nanovid microscopy). Effects of calcium-induced differentiation in cultured epithelial cells. Biophysical Journal 65:2021-2040

55. **Feder TJ, Brust-Mascher, I., Slattery, J.P., Baird, B., & Webb, W.W.** 1996 Constrained Diffusion or Immobile Fraction on Cell Surfaces: A New Interpretation. Biophysical Journal 70:2767-2773

56. **Austin RH, Chan SS, Jovin TM** 1979 Rotational diffusion of cell surface components by time-resolved phosphorescence anisotropy. Proc Natl Acad Sci U S A 76:5650-4.

57. **Saffman PG, Delbrück M** 1975 Brownian motion in biological membranes. Proceedings of the National Academy of Science (USA) 72:3111-3113

58. **Song J, Hagen GM, Roess DA, Pecht I, Barisas BG** 2002 The mast cell function-associated antigen and its interactions with the type I Fcepsilon receptor. Biochemistry. 41:881-9

59. **Dietrich C, Yang B, Fujiwara T, Kusumi A, Jacobson K** 2002 Relationship of lipid rafts to transient confinement zones detected by single particle tracking. Biophys J 82:274-84.

60. **Song J, Hagen GM, Roess DA, Pecht I, Barisas BG** 2002 The mast cell function-associated antigen and its interactions with the type I Fcε receptor. Biochemistry 41:881-9

61. **Jovin T, Bartholdi M, Vaz W, Austin RH** 1981 Rotational diffusion of biological macromolecules by time-resolved delayed luminescence (phosphorescence, fluorescence) anisotropy. Annals New York Academy of Sciences 366:176-196

62. **Keutmann HT, McIlroy PJ, Bergert ER, Ryan RJ** 1983 Chemically deglycosylated human chorionic gonadotropin subunits: Characterization and biological properties. Biochemistry 22:3067-3072

63. **Fernandez LM, Puett D** 1996 Lys^{583} in the third extracellular loop of the lutropin/choriogonadotropin receptor is critical for signaling. J Biol Chem 271:925-30

64. **Ryu K-S, Gilchrist RL, Ji I, Kim S-J, Ji TH** 1996 Exoloop 3 of the luteinizing hormone/chorionic gonadotropin receptor: Lys583 is essential and irreplaceable for human chorionic gonadotropin (hCG)-dependent receptor activation but not high affinity hCG binding. Journal of Biological Chemistry 271:7301-7304

65. **Young RM, Arnette JK, Roess DA, Barisas BG** 1994 Quantitation of fluorescence energy transfer between cell surface proteins via fluorescence donor photobleaching kinetics. Biophysical Journal 67:881-888

66. **Luborsky J, Slater W, Behrman H** 1984 Luteinizing hormone (LH) receptor aggregation: modification of ferritin-LH binding and aggregation by prostaglandin $F_{2\alpha}$ and ferritin-LH. Endocrinology 115:2217-2225

67. **Amsterdam A, Berkowitz A, Nimrod A, Kohen F** 1980 Aggregation of luteinizing hormone receptors in granulosa cells: a possible mechanism for desensitization to the hormone. Proc. Nat. Acad. Sci. (USA) 77:3440-3445

68. **Podestá EJ, Solano AR, Sánchez ML** 1986 Luteinizing hormone triggers two opposite regulatory pathways through an initial common event, receptor aggregation. Endocrinology 119:989-997

69. **Roess DA, Horvat RD, Munnelly H, Barisas BG** 2000 Luteinizing hormone receptors are self-associated in the plasma membrane. Endocrinology 141:4518-23

70. **Hebert TE, Loisel TP, Adam L, Ethier N, St. Onge S, Bouvier M** 1998 Functional rescue of a constitutively desensitized β_2AR through receptor dimerization. Biochemical Journal 330:287-93

71. **Cvejic S, Devi LA** 1997 Dimerization of the δ opioid receptor: Implication for a role in receptor internalization. J Biol Chem 272:26959-26964

72. **Maggio R, Vogel Z, Wess J** 1993 Coexpression studies with mutant muscarinic/adrenergic receptors provide evidence for intermolecular "cross-talk" between G-protein-linked receptors. Neurobiology 90:3101-3107

73. **Freedman NJ, Lefkowitz RJ** 1996 Desensitization of G-protein coupled receptors. Recent Progress in Hormone Research 51:319-353

74. **Hunzicker-Dunn M, Day SL, Abramowitz J, Birnbaumer L** 1979 Ovarian responses of pregnant mare serum gonadotropin- and human chorionic gonadotropin-primed rats: desensitizing luteolytic, and ovulatory effects of a single dose of human chorionic gonadotropin. Endocrinology 105:442-451

75. **Hunzicker-Dunn M, Birnbaumer L** 1981 Studies on the mechanism of luteinizing hormone-induced desensitization of the rabbit follicular adenylyl cyclase system *in vitro*. Endocrinology 109:345-351

76. **Jonassen JA, Richards JS** 1980 Granulosa cell desensitization: effects of gonadotropins on antral and preantral follicles. Endocrinology 106, no. 4:1786-1794

77. **Dix CJ, Schumacher M, Cooke BA** 1982 Desensitization of tumor Leydig cells by lutropin: evidence for uncoupling of the lutropin receptor from the guanine nucleotide-binding protein. Biochemistry Journal 202:739-745

78. **Rebois RV, Fishman PH** 1986 Gonadotropin-mediated desensitization in a murine Leydig tumor cell line does not alter the regulatory and catalytic components of adenylate cyclase. Endocrinology 118:2340-2347

79. **Hunzicker-Dunn M, Birnbaumer L** 1976 Adenylyl cyclase activities in ovarian tissues. II. regulation of responsiveness to LH, FSH, and PGE_1 in the rabbit. Endocrinology 99:185-197

80. **Zor U, Shentzer P, Azrad A, Sairam MR, Amsterdam A** 1984 Deglycosylated luteinizing hormone LH prevents desensitization of cyclic adenosine monophosphate response by LH: dissociation between receptor uncoupling and down-regulation. Endocrinology 114:2143-2147

81. **Hunzicker-Dunn M, Birnbaumer L** 1976 Adenylyl cyclase activities in ovarian tissues. III. regulation of responsiveness to LH, FSH, and PGE_1 in the prepubertal, cycling, pregnant, and pseudopregnant rat. Endocrinology 99:198-210

82. **Downs SM, Hunzicker-Dunn M** 1995 Differential regulation of oocyte maturation

and cumulus expansion in the mouse oocyte-cumulus cell complex by site-selective analogs of cyclic adenosine monophosphate. Developmental Biology 172:72-85

83. **Niswender GD, Roess DA, Sawyer HR, Silvia WJ, Barisas BG** 1985 Differences in the lateral mobility of receptors for luteinizing hormone (LH) in the luteal cell plasma membrane when occupied by ovine LH versus human chorionic gonadotropin. Endocrinology 116:164-169

84. **Roess DA, Rahman NA, Kenny N, Barisas BG** 1992 Molecular dynamics of luteinizing hormone receptors on rat luteal cells. Biochim Biophys Acta 1137:309-316

85. **Horvat RD, Nelson S, Clay CM, Barisas BG, Roess DA** 1999 Intrinsically fluorescent luteinizing hormone receptor demonstrates hormone-driven aggregation. Biochem. Biophys. Res. Comm. 255:382-385

86. **Rietvild A, Simons K** 1998 The differential miscibility of lipids as the basis for the formation of functional membrane rafts. Biochimica et Biophysica Acta 1376:467-479

87. **Waugh MG, Lawson D, Hsuan JJ** 1999 Epidermal growth factor receptor activation is localized within low-buoyant density, non-caveolar membrane domains. Biochemical Journal 337:591-597

88. **Lang ML, Shen L, Wade WF** 1999 γ -Chain dependent recruitment of tyrosine kinases to membrane rafts by the human IgA receptor FcαR. The Journal of Immunology 163:5391-5398

89. **Lemmon M, Flanagan J, Treutlein H, Zhang J, Engleman D** 1992 Sequence

specificity in the dimerization of transmembrane alpha-helices. Biochemistry 31:12719-12725

90. **Guo W, Shi L, Javitch JA** 2003 The fourth transmembrane segment forms the interface of the dopamine D2 receptor homodimer. The Journal of Biological Chemistry 278:4385-4388

91. **Hunzicker-Dunn M, Barisas BG, Song J, Roess DA** 2003 Membrane organization of luteinizing hormone receptors differs between actively signaling and desensitized receptors. J. Biol. Chem. 278:42744-42749

92. **Harmatz D, Ji TH, Middaugh CR** 1985 Aggregation state of the gonadotropin receptor. Biochemical and Biophysical Research Communications 127:687-692

93. **Ilangumaran S, Hoessli DC** 1998 Effects of cholesterol depletion by cyclodextrin on the sphingolipid microdomains of the plasma membrane. Biochemistry Journal 335:433-40

94. **Pralle A, Keller P, Florin E, Simons K, Hörber JKH** 2000 Sphingolipid-cholesterol rafts diffuse as small entities in the plasma membrane of mammalian cells. Journal of Cell Biology 148:997-1008

95. **Gidwani A, Holowka D, Baird B** 2001 Fluorescence anisotropy measurements of lipid order in plasma membranes and lipid rafts from RBL-2H3 mast cells. Biochemistry 40:12422-12429

96. **Harder T, Simons K** 1997 Caveolae, DIGs, and the dynamics of sphingolipid-cholesterol microdomains. Current Opinion in Cell Biology 9, no. 4:534-542

97. **Xiao Z, Devreotes PN** 1997 Identification of detergent-resistant plasma membrane

microdomains in dictyostelium: enrichment of signal transduction proteins. Molecular Biology of the Cell 8:855-869

98. **Hiol A, Davey P, Osterhout J, et al.** 2003 Palmitoylation regulates regulators of G-protein signaling (RGS) 16 function. J Biol Chem 278:19301-19308

99. **Roess DA, Brady CJ, Barisas BG** 2000 Biological function of the LH receptor is associated with slow receptor rotational diffusion. Biochimica et Biophysica Acta. 1464:242-50

100. **Christian AE, Haynes MP, Phillips MC, Rothblat GH** 1997 Use of cyclodextrins for manipulating cellular cholesterol content. J Lipid Res 38:2264-2272

101. **Kilsdonk EPC, Yancey PG, Stoudt GW, et al.** 1995 Cellular cholesterol efflux mediated by cyclodextrins. J Biol Chem 270:17250-17256

102. **Murase K, Fujiwara T, Umemura Y, et al.** 2004 Ultrafine membrane compartments for molecular diffusion as revealed by single molecule techniques. Biophys J 86:4075-4093

103. **Daumas F, Destainville N, Millot C, Lopez A, Dean D, Salomé L** 2003 Confined diffusion without fences of a G protein coupled receptor as revealed by single particle tracking. The Biophysical Journal 84:356-366

104. **Saxton MJ** 1997 Single-particle tracking: the distribution of diffusion coefficients. Biophys J 72:1744-1753

105. **Roess DA, Smith SML** 2003 Self-association and raft localization of functional luteinizing hormone receptors. Biol Reprod 69:1765-1770

106. **Bramley TA, Ryan RJ** 1978 Interactions of gonadotropins with corpus luteum

membranes. II. The identification of two distinct surface membrane fractions from superovulated rat ovaries. Endocrinology 103:796-804

107. **Brown DA, London E** 2000 Structure and Function of Sphingolipid- and Cholesterol-rich Membrane Rafts. J. Biol. Chem. 275:17221-17224

108. **Kawate N, Peegel H, Menon K** 1997 Role of palmitoylation of conserved cystine residues of luteinizing hormone/human choriogonadotropin receptors in receptor down-regulation. Molecular and Cellular Endocrinology 127:211-219

109. **Munshi UM, Peegel H, Menon KM** 2001 Palmitoylation of the luteinizing hormone/human chorionic gonadotropin receptor regulates receptor interaction with the arrestin-mediated internalization pathway. Eur. J. Biochem. 268:1631-1639

110. **Lei Y, Hagen G, Smith S, Barisas BG, Roess D** 2005 Chimeric GnRH-LH receptors and LH receptors lacking C-terminus palmitoylation sites do not localize to plasma membrane rafts. Biochem Biophys Res Commun 337:430-434

111. **Loisel TP, Adam L, Hebert TE, Bouvier M** 1996 Agonist stimulation increases the turnover rate of beta2 AR-bound palmitate and promotes receptor depalmitoylation. Biochemistry 35:15923-15932

112. **Qanbar R, Bouvier M** 2003 Role of palmitoylation/depalmitoylation reactions in G-protein-coupled receptor function. Pharmacological Therapeutics 97:1-33

113. **Dykstra M, Cherukuri A, Sohn H, Tzeng S, Pierce S** 2003 Location is everything: lipid rafts and immune cell signaling. Annual Review of Immunology 21:457-481

114. **Harder T** 2001 Raft membrane domains and immunoreceptor functions. Advances in Immunology 77:45-92

115. **Young RM, Holowka D, Baird B** 2003 A lipid raft environment enhances Lyn kinase activity by protecting the active site tyrosine from dephosphorylation. J. Biol. Chem. 278:20746-20752

116. **Moffett S, Brown DA, Linder ME** 2000 Lipid-dependent targeting of G-proteins into rafts. Journal of Biological Chemistry 275:2191-2198

117. **Rybin VO, Xu X, Lisanti MP, Steinberg SF** 2000 Differential targeting of beta-adrenergic receptor subtypes and adenylyl cyclase to cardiomyocyte caveolae. A mechanism to functionally regulate the cAMP signaling pathway. J. Biol. Chem. 275:41447-41457

118. **Ostrom RS, Gregorian C, Drenan RM, Xiang Y, Regan JW, Insel PA** 2001 Receptor number and caveolar co-localization determine receptor coupling efficiency to adenylyl cyclase. J. Biol. Chem. 276:42063-42069

119. **Ostrom RS, Post SR, Insel PA** 2000 Stoichiometry and compartmentation in G protein-coupled receptor signaling: implications for therapeutic interventions involving Gs. J Pharmacol Exp Ther 294:407-412

120. **Varma R, Mayor S** 1998 GPI-anchored proteins are organized in submicron domains at the cell surface. Nature 394, no. 20:798-801

121. **Stulnig TM, Waldhauls, Werner** 1997 Signal Transduction via Glycosyl Phosphatidylinositol-anchored Proteins in T Cells is Inhibited by Lowering Cellular Cholesterol. J Biol Chem 272:19242-19247

122. **Huby RDJ, Dearman RJ, Kimber I** 1999 Intracellular phosphotyrosine induction by major histocompatibility complex class II requires co-aggregation with membrane

rafts. Journal of Biological Chemistry 274, no. 32:22591-6

123. **Sako Y, Kusumi A** 1994 Compartmentalized structure of the plasma membrane for receptor movements as revealed by a nanometer-level motion analysis. Journal of Cell Biology. 125:1251-1264

124. **Ritchie K, Iino R, Fujiwara T, Murase K, Kusumi A** 2003 The fence and picket structure of the plasma membrane of live cells as revealed by single molecule techniques (review). Molecular Membrane Biology 20:13-18

125. **Roess DA, Niswender GD, Barisas BG** 1988 Cytochalasins and colchicine increase the lateral mobility of human chorionic gonadotropin-occupied luteinizing hormone receptors on ovine luteal cells. Endocrinology 122:261-269

126. **Sagi-Eisenberg R, Lieman H, Pecht I** 1985 Protein kinase C regulation of the receptor-coupled calcium signal in histamine-secreting rat basophilic leukaemia cells. Nature. 313:59-60

127. **Beaven M, Moore J, Smith G, Hesketh T, Metcalfe J** 1984 The calcium signal and phosphatidylinositol breakdown in 2H3 cells. Journal of Biological Chemistry 259:7137-7142

128. **Guo N, Her G, Reinhold V, Brennan M, Siraganian R, Ginsburg V** 1989 Monoclonal antibody AA4, which inhibits binding of IgE to high affinity receptors on rat basophilic leukemia cells, binds to novel α-galactosyl derivatives of ganglioside G_{D1b}. Journal of Biological Chemistry 264:13267-13272

129. **Ortega E, Licht A, Biener Y, Pecht I** 1990 A glycolipid-specific monoclonal antibody modulates Fcε receptor stimulation of mast cells. Molecular Immunology

27:1269-1277

130. **Stephan V, Guo N, Ginsburg V, Siraganian R** 1991 Immunoprecipitation of membrane proteins from rat basophilic leukemia cells by the antiganglioside monoclonal antibody AA4. The Journal of Immunology 146:4271-4277

131. **Kitani S, Berenstein E, Mergenhagen S, Tempst P, Siraganian R** 1991 A cell surface glycoprotein of rat basophilic leukemia cells close to the high affinity IgE receptor (FcγRI). Journal of Biological Chemistry 266:1903-1909

132. **Hamawy M, Oliver C, Siriganian R** 1992 Inhibition of IgE binding to RBL-2H3 cells by a monoclonal antibody (BD6) to a surface protein other than the high affinity IgE receptor. The Journal of Immunology 148:524-531

133. **Ortega E, Pecht I** 1988 A monoclonal antibody that inhibits secretion from rat basophilic leukemia cells and binds to a novel membrane component. The Journal of Immunology 141:4324-4332

134. **Guthmann MD, Tal M, Pecht I** 1995 A new member of the C-type lectin family is a modulator of the mast cell secretory response. International Archives of Allergy and Immunology 107:82-86

135. **Xu R, Abramson J, Fridkin M, Pecht I** 2001 SH2 domain-containing inositol polyphosphate 5'-phosphatase is the main mediator of the inhibitory action of the mast cell function-associated antigen. J Immunol 167:6394-402

136. **Xu R, Pecht I** 2001 The protein tyrosine kinase syk activity is reduced by clustering the mast cell function-associated antigen. Eur J Immunol 31:1571-81

137. **Jurgens L, Arndt-Jovin D, Pecht I, Jovin TM** 1996 Proximity relationships

between the type I receptor for Fc epsilon (Fc epsilon RI) and the mast cell function-associated antigen (MAFA) studied by donor photobleaching fluorescence resonance energy transfer microscopy. Eur J Immunol 26:84-91

138. **Song J, Hagen GM, Roess DA, Pecht I, Barisas BG** 2002 The mast cell function-associated antigen and its interactions with the type I Fcepsilon receptor. Biochemistry 41:881-9

139. **Field KA, Holowka D, Baird B** 1995 Fc-epsilon-RI-mediated recruitment of p53/56lyn to detergent-resistant membrane domains accompanies cellular signaling. Proceedings of the National Academy of Science (USA) 92:9201-9205

140. **Carsten ME, Eisen HN** 1953 The interaction of dinitrobenzene derivatives with bovine serum albumin. Journal of the American Chemical Society 75:4451-4456

141. **Johnson GD, Holborow EJ** 1986 Preparation and use of flourochrome conjugates. In: Weir DM (ed) Handbook of Experimental Immunology, 14th ed. Blackwell Scientific Publications, Boston, pp 28.1-28.21

142. **Philpott CJ, Rahman NA, Kenny N, Barisas BG, Roess DA** 1995 Rotational dynamics of luteinizing hormone receptors on bovine and ovine luteal cell plasma membranes. Biology of Reproduction 53:645-650

143. **Barisas BG, Wade WF, Jovin TM, Arndt-Jovin D, Roess DA** 1999 Dynamics of molecules involved in antigen presentation: effects of fixation. Mol Immunol 36:701-8.

144. **Johnson P, Garland PB** 1981 Depolarization of fluorescence depletion. A microscopic method for measuring rotational diffusion of membrane proteins on the

surface of a single cell. FEBS Lett 132:252-6.

145. **Song J, Hagen G, Smith SM, Roess DA, Pecht I, Barisas BG** 2002 Interactions of the mast cell function-associated antigen with the type I Fcepsilon receptor. Mol Immunol 38:1315-21

146. **Field KA, Holowka D, Baird B** 1999 Structural aspects of the association of FcεRI with detergent-resistant membranes. Journal of Biological Chemistry 274:1753-8

147. **Smith SML, Lei Y, Liu J, et al.** 2006 Luteinizing hormone receptors translocate to plasma membrane microdomains followingbinding of human chorionic gonadotropin. Endocrinology 147:1789-1795

148. **Ortega E, Schneider H, Pecht I** 1991 Possible interactions between the Fc epsilon receptor and a novel mast cell function-associated antigen. Int Immunol 3:333-42

149. **Licht A, Abramson J, Pecht I** 2006 Co-clustering activating and inhibitory receptors: impact at varying expression levels of the latter. Immunol Lett 104:166-70

150. **Licht A, Pecht I, Schweitzer-Stenner R** 2005 Regulation of mast cells' secretory response by co-clustering the Type 1 Fcepsilon receptor with the mast cell function-associated antigen. Eur J Immunol 35:1621-33

151. **Holowka D, Gosse JA, Hammond AT, et al.** 2005 Lipid segregation and IgE receptor signaling: a decade of progress. Biochim Biophys Acta 1746:252-9

LIST OF ABBREVIATIONS

A_2IgE: Anti-DNP Immunoglobulin E

AC: Adenylyl cyclase

ATP: Adenosine triphosphate

BSS: Hank's balanced salt solution

cAMP: Cyclic adenosine monophosphate

CFP: Cyan fluorescent protein

CHO: Chinese hamster ovary

D: Diffusion coefficient

Da: Dalton (molecular weight)

DAG: Diacylglycerol

DMEM: Dulbecco's modified minimum essential medium

DNP_{14}-BSA: Bovine serum albumen coupled to dinitrophenol

EGFR: Epidermal growth factor receptor

Fab: Fraction antigen binding

FBS: Fetal bovine serum

FcεRI: High affinity receptor for IgE

FITC: Fluorescein isothiocyanate

FMPP: Familial male-limited precocious puberty

FPR: Fluorescence photobleaching recovery

FRET: Fluorescence resonance energy transfer

G418: Geneticin

G63:	Monoclonal antibody specific for MAFA
GDP:	Guanosine diphosphate
GFP:	Green fluorescent protein
G_i:	Inhibitory G protein
GM1:	Membrane ganglioside
GnRH:	Gonadotropin releasing hormone
GPCR:	G protein-coupled receptor
GPI:	Glycosylphosphatidylinositol
G_s:	Stimulatory G protein
GTP:	Guanosine triphosphate
hCG:	Human chorionic gonadotropin
hLHR:	Human luteinizing hormone receptor
IP_3:	Inositol 1,4,5-triphosphate
ITAM:	Immunoreceptor tyrosine activation motif
ITIM:	Immunoreceptor tyrosine inhibition motif
LH:	Luteinizing hormone
mAb:	Monoclonal antibody (intact)
MAFA:	Mast cell function-associated antigen
MβCD:	Methyl-β-cyclodextrin
MEM:	Minimum essential medium
PAGE:	Polyacrylamide gel electrophoresis
PBS:	Phosphate buffered saline

PIP_3:	Phosphatidylinositol triphosphate
PKA:	Protein kinase A
PKC:	Protein kinase C
PLCγ:	Phospholipase C gamma
RBL-2H3:	Rat basophilic leukemia-derived cell line
RCT:	Rotational correlation time
rLHR:	Rat luteinizing hormone receptor
SDS:	Sodium dodecylsulfate
TNFR:	Tumor necrosis factor receptor
TPA:	Time-resolved phosphorescence anisotropy
TrITC:	Tetramethyl rhodamine isothiocyanate
VFP:	Visible fluorescent protein
YFP:	Yellow fluorescent protein